

A UNITED STATES
DEPARTMENT OF
COMMERCE
PUBLICATION

TELECOMMUNICATIONS

Technical Memorandum

U.S. DEPARTMENT OF COMMERCE
OFFICE OF TELECOMMUNICATIONS
Institute for Telecommunication Sciences

Interference Predictions for VHF/UHF Air Navigation Aids

(Supplement to IER 26-ITSA 26 and ERL 138-ITS 95)

G.D. Gierhart

M.E. Johnson

**BOULDER,
COLORADO**

January 1971

U.S. DEPARTMENT OF COMMERCE
OFFICE OF TELECOMMUNICATIONS
Institute for Telecommunication Sciences

INTERFERENCE PREDICTIONS
FOR VHF/UHF AIR NAVIGATION AIDS
(SUPPLEMENT TO IER 26-ITSA 26 and ERL 138-ITS 95)

G. D. Gierhart
M. E. Johnson

Institute for Telecommunication Sciences
Boulder, Colorado
January 1971



FOREWORD

This report was prepared for the Spectrum Plans and Programs Branch, Frequency Management Division, Systems Research and Development Service, Federal Aviation Administration, under Contract No. FA 68-WAI-145. The views presented are not necessarily those of the FAA and do not reflect FAA Policy. This report does not constitute a standard, specification, or regulation.

Technical memoranda are used to insure prompt dissemination of special information that has been developed in response to a specific need for a sponsoring agency. These documents are in the public domain since they are issued as official government writing, but are considered to be unpublished since they are not printed for wide public distribution. Copies of this particular Technical Memorandum are sold for \$3.00 each (\$0.95, microfiche) by the National Technical Information Service (NTIS), Operations Division, Springfield, Va. 22151. One orders by using the accession number given on the cover. Any abstracting, citing or reproduction of this document should be accompanied by the information required to obtain it from NTIS.

TABLE OF CONTENTS

	Page
LIST OF FIGURES	iv
LIST OF TABLES	v
ABSTRACT	1
1. INTRODUCTION	1
2. RADIATION PATTERNS	2
2.1 ILS Localizer	3
2.2 TACAN and DME	7
3. PROPAGATION MODELS	14
3.1 L_{cr} Models	14
3.2 V_{lt} Models	17
3.3 V_{st} Models	22
4. ILS LOCALIZER STATION SEPARATIONS	24
5. ATTENUATION CURVES	27
6. SERVICE VOLUME CURVES	42
7. REFERENCES	51
APPENDIX A. ERRATA FOR PREVIOUS REPORTS	54
A.1 ESSA Technical Report IER 26-ITSA 26	54
A.2 ESSA Technical Report ERL 111-ITS 79	54

LIST OF FIGURES

		Page	
1.	ILS localizer twin-tee array antenna pattern.	5	
2.	ILS localizer multi-dipole array pattern.	6	
3.	ΔG vs. elevation angle.	10	
4.	Direct ray elevation angles.	11	
5.	Gain vs. elevation angle; TACAN, RTA-2.	13	
6.	$V_{lt}(95)$ for ILS localizer and VOR.	20	
7.	$V_{lt}(95)$ for TACAN.	21	
8.	L_{cr} and $V_{lt}(95)$ vs. distance; ILS localizer and VOR.	26	
<u>9-20 Attenuation greater than free space vs. distance</u>			
	<u>Facility or</u> <u>frequency</u>	<u>Antenna</u> <u>$L_{cr}/V_{lt}/V_{st}$</u>	
9.	1150 MHz	Isotropic $h_1 = 0$ to 35 ft 69/70/No	30
10.	1150 MHz	Isotropic $h_1 = 0$ to 35 ft 69/70/70	31
11.	1200 MHz	Isotropic 69/70/70	32
12.	TACAN	RTA-2 62 ΔG /70/67	33
13.	TACAN	RTA-2 69 ΔG /70/67	34
14.	TACAN	RTA-2 $h_1 = 0$ to 100 ft 69/70/70	35
15.	TACAN	URN-3 62/62/67	36
16.	TACAN	URN-3 62/70/67	37
17.	TACAN	URN-3 69/70/67	38
18.	118 MHz	Isotropic 69/70/67	39
19.	VOR	4-loop 62/62/67	40
20.	VOR	4-loop 62/70/67	41

21-27 Service volumes without interference

	<u>Facility or frequency</u>	<u>Antenna</u>	<u>$L_{cr} / V_{lt} / V_{st}$</u>	
21.	DME	DME	62 Δ G/70/67	44
22.	1200 MHz	Isotropic	69/70/70	45
23.	TACAN	RTA-2	62 Δ G/70/67	46
24.	TACAN	URN-3	62/62/67	47
25.	TACAN	URN-3	62/70/67	48
26.	118 MHz	Isotropic	69/70/67	49
27.	VOR	4-loop	62/62/67 62/70/67	50

A. 1-A. 3 Normalized D/U for co-channel ILS localizers

	<u>Altitude</u>	
A. 1	2,000 ft	55
A. 2	3,000 ft	56
A. 3	4,000 ft	57
A. 4	Service Volumes for VOR, DU(95) = 32 dB	58

LIST OF TABLES

1.	Characteristics of ILS Localizers	4
2.	ILS Localizer C_f Values in Decibels	8
3.	Propagation Model Codes	15
4.	V_{lt} Models	19
5.	ILS Localizer Station Separations	25
6.	Reference Power Equivalents	42

INTERFERENCE PREDICTIONS
FOR VHF/UHF AIR NAVIGATION AIDS
(SUPPLEMENT TO IER 26-ITSA 26 and ERL 138-ITS 95)

G.D. Gierhart and M.E. Johnson

This report supplements information previously developed by the authors on interference predictions for VHF/UHF air navigation aids. Included are (a) radiation patterns needed to adapt curves previously developed for the Instrument Landing System (ILS) Localizer and Tactical Air Navigation (TACAN) to new equipment types, (b) comparisons of the propagation models used for predictions made from 1962 to the present, (c) propagation information in a different form, i.e. attenuation greater than free space for Distance Measuring Equipment (DME), TACAN and VHF Omni-range (VOR), (d) DME, TACAN and VOR service volume without interference curves for equipment configurations not previously considered, and (e) an errata list for earlier ESSA Technical Reports.

Key words: DME, ILS, interference, navigation aids, propagation, TACAN, transmission loss, VOR.

1. INTRODUCTION

This report for the Federal Aviation Administration (FAA) concerns work by the Institute for Telecommunication Sciences (ITS) during November, 1969 to July, 1970. Much of the information contained herein was previously provided to the FAA in preliminary form by letter reports.

This report supplements earlier ESSA Technical Reports (Gierhart and Johnson, 1967, 1969a) on the same subject. It provides (a) radiation patterns needed to adapt curves previously developed for the Instrument Landing System (ILS) Localizer and Tactical Air Navigation (TACAN) to new facility equipment (sec. 2), (b) comparisons of the propagation models used for predictions made from 1962 to 1970

(sec's, 3 and 4), (c) propagation information as attenuation greater than free space basic transmission loss (sec. 5) for Distance Measuring Equipment (DME), TACAN and VHF Omnirange (VOR), (d) DME, TACAN, and VOR service volume without interference for equipment configurations not previously considered (sec. 6), and (e) an errata list for earlier ESSA Technical Reports (app. A).

The facilities treated operate at frequencies from about 0.1 to 1 GHz. Propagation of radio frequency energy at these frequencies is affected by the lower, non-ionized atmosphere (troposphere), specifically by variations in the refractive index and terrain along and in the vicinity of the great-circle path between transmitter and receiver. Time and space variations of received signal and interference ratios are best expressed statistically. The methods used to characterize propagation in these predictions follow procedures used by ITS to predict the effects of terrain and atmosphere on the variability of field strength, and on the performance of radio systems (Barsis et al., 1970; Gierhart et al., 1970; Gierhart and Johnson, 1967, 1969a, 1969b; Johnson, 1967; Longley and Rice, 1968; Longley and Reasoner, 1970; Rice et al., 1967).

These methods use the concept of transmission loss, which is the ratio (usually expressed in dB) of the total power radiated from the transmitting antenna to the power that would be available at the receiving antenna terminals if there were no circuit losses other than those associated with the radiation resistance of the receiving antenna.

2. RADIATION PATTERNS

Previous studies were limited to specific facility antenna types. Information given in this section can be used to extend the results previously obtained to some particular new equipment types.

2.1 ILS Localizer

Service range curves previously developed for the ILS localizer are in terms of a normalized desired-to-undesired signal ratio (Gierhart and Johnson, 1969a, sec. 5.2). Use of these curves requires that the radiation characteristics of the particular desired and undesired facilities are considered. This includes an allowance for the azimuth characteristic of the undesired facility and compensation for the relative effective radiated powers of the two facilities by a combination factor, C_f .

Relevant characteristics of ILS localizers are summarized in table 1. Standard, directional, Mark I (referred to as "Low Cost" in previous reports) and AN/MRN-7 equipment types were considered previously and the azimuth patterns of their antenna are given in Gierhart and Johnson (1969a, figs. 1, 2 and 3). Azimuth patterns for the carrier portion of the twin-tee (AIL 55-E and F) and multi-dipole (Wilcox 412) arrays are shown in figures 1 and 2. These figures give the gain factor G required by Gierhart and Johnson [1969a, eqn. (1)]. Information made available via the FAA (AIL; Hollm, 1968; Wilcox) was used to estimate the system parameters required to calculate C_f values and develop azimuth patterns for the AIL 55-E and F and Wilcox 412 equipment types. The value C_f is defined by

$$C_f = P_D - P_U + A_D - A_U + H_D - H_U \quad (1)$$

where

- P_D = carrier power radiated by desired facility in dBW,
- P_U = carrier power radiated by undesired station in dBW,
- A_D = free-space antenna gain referred to an isotropic radiator for the main lobe of the desired station carrier antenna array, in dB;

Table 1. Characteristics of ILS Localizers

	Standard	Directional	Mark I	AN/MRN-7	AIL 55-E&F	Wilcox 412
Radiated power ^(a)	20 dBW	20 dBW	10 dBW	7 dBW	3 dBW ^(b)	10 dBW ^(c)
Array type	8-loop	V-ring	V-ring	12-dipole	Twin-tee	Multi-dipole
Antenna gain ^(d)	4 dB	12 dB	12 dB	18 dB	12 dB ^(e)	12 dB ^(f)
Array height above ground	5.5 ft	7.5 ft	7.5 ft	4.5 ft	5.5 ft ^(g)	5.5 ft

(a) Radiated power refers to the total carrier power radiated from the array.

(b) The modulated carrier output of the localizer transmitter 1 modulator unit type 55-120 is given as 4 W or 6 dBW (AIL, p. 17). However, this value includes sideband as well as carrier power and does not include losses associated with the transmission line. A 3 dB reduction (6 to 3 dBW) was made to allow for these factors.

(c) The localizer transmitter is capable of providing 30 W or 14.8 dBW of rf power (Wilcox, p. 23). However, a reduction in power is expected because of losses associated with the modulator (Wilcox, p. 6) rf distribution network (Wilcox, p. 22). A 4.8 dB reduction was made (14.8 to 10 dBW) to allow for these factors.

(d) Antenna gain refers to the main lobe free-space gain associated with the radiation of carrier power and is with reference to an isotropic radiator.

(e) Taken as equal to that of the V-ring as suggested by Hollm (1968).

(f) Taken as 12 dB in accordance with the value added to Wilcox (p. 20) in Mr. Johnson's (FAA) copy.

(g) Height is adjustable from 4 to 10 ft with higher elevations possible. A nominal or typical height of 5.5 ft is assumed.

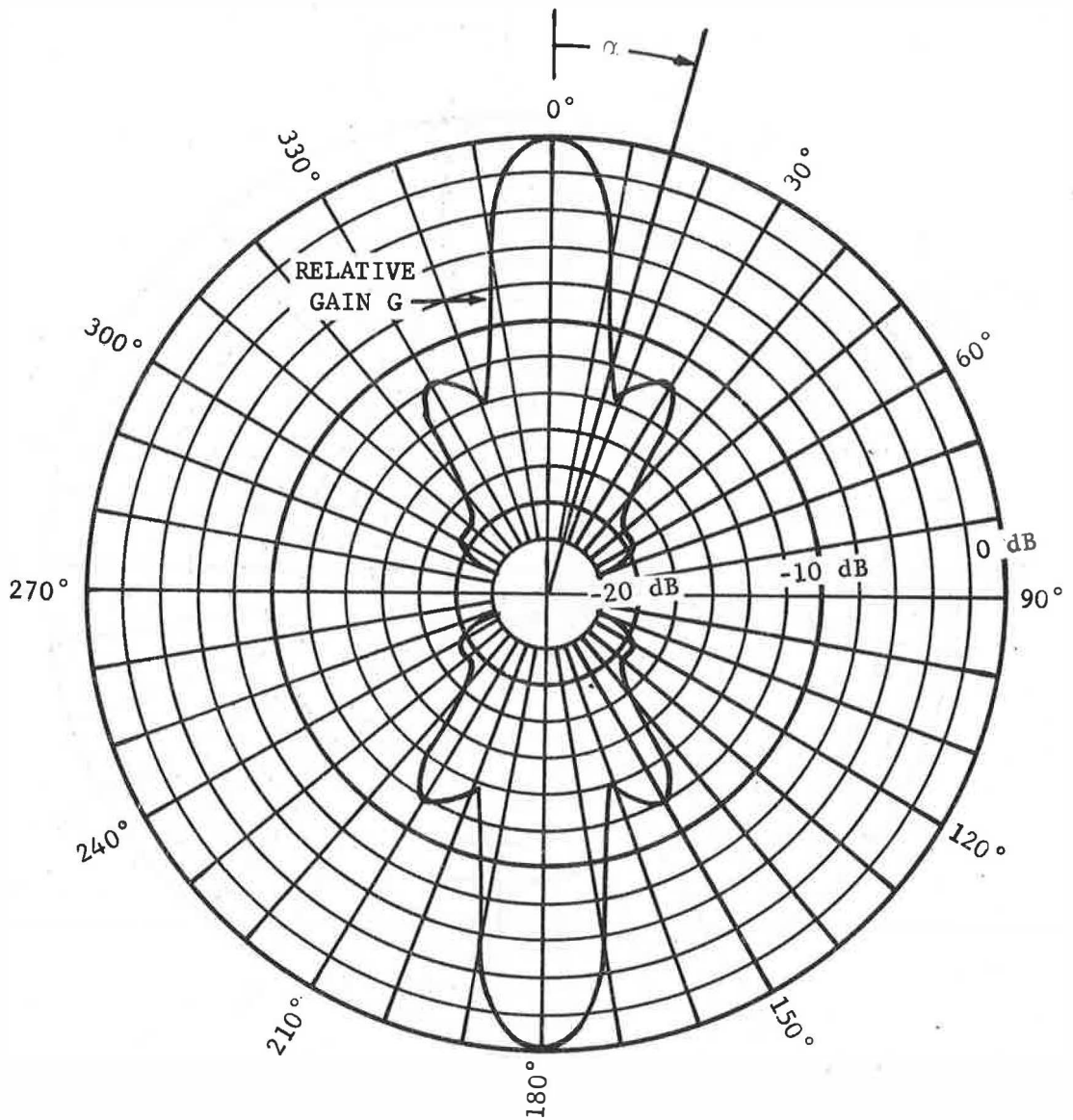


Figure 1. ILS localizer twin-tee array antenna pattern. Free-space gain for the carrier portion of the array in the azimuth plane is in decibels relative to the main-lobe maximum. The gain of the main-lobe maximum is taken as 12 dB greater than an isotropic radiator (table 1). This pattern was derived from fig. 3-12 of Hollm (1968) by converting relative field strength (dimensionless voltage ratio) to relative gain in dB and smoothing the resulting pattern to obtain symmetry about the main-lobe.

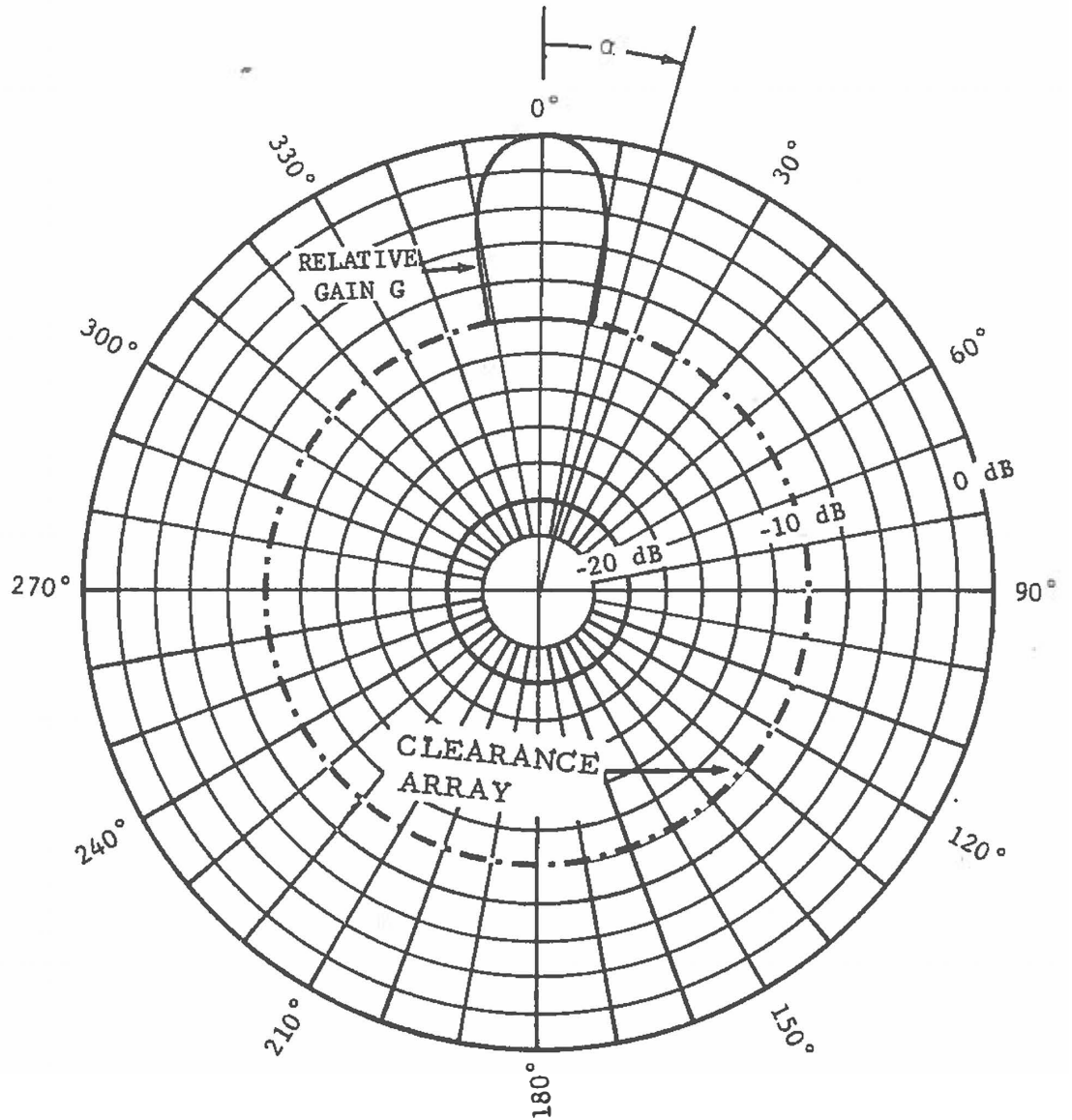


Figure 2. ILS localizer multi-dipole array antenna pattern. Free-space gain for the carrier portion of the array in the azimuth plane is in decibels relative to the main-lobe maximum. The gain of the main-lobe maximum is taken as 12 dB greater than an isotropic radiator (table 1). A 3 dB beamwidth of 18° inferred from Wilcox (p. 7) was used for the main-lobe and the remainder of the pattern was taken as 10 dB less than the main-lobe maximum (Wilcox, p. 20).

A_U = antenna gain similar to A_D but for undesired station,

H_D = height gain factor for desired station, i. e.,

H_D = 0 dB for ILS array height of 5.5 ft (8-loop, twin-tee, multi-dipole),

H_D = 1.5 dB for ILS array height of 7.5 ft (V-ring),

H_D = -1.5 dB for ILS array height of 4.5 ft (AN/MRN-7);

and

H_U = height gain factor for undesired station, i. e.,

H_U = 0 dB for ILS array height of 5.5 ft

(8-loop, twin-tee, multi-dipole) and VOR,

H_U = 2.5 dB for ILS array height of 7.5 ft (V-ring),

H_U = -0.5 dB for ILS array height of 4.5 ft (AN/MRN-7).

Values of C_f required for Gierhart and Johnson [1969a, eqn. (1)] are given in table 2. These values were calculated using the parameter values of table 1 and Gierhart and Johnson (1969a, table 3 for VOR) in (1). Table 2 is an expanded version of Gierhart and Johnson (1969a, table 6).

2.2 TACAN and DME

Service volume without interference curves (sec. 5; Gierhart and Johnson, 1967, fig. 9) and attenuation greater than free-space curves (sec. 4) developed for a TACAN facility with a URN-3 antenna may be used in cases where a RTA-2 (FAA, 1963, sec. 3.3.3), DME (FAA, 1967, sec. 3.5) or isotropic antenna is involved if an adjustment is made. The required adjustment depends on the relative antenna gain applicable at the elevation angle required to illuminate a particular aircraft location.

Relative gain ΔG versus elevation angle is shown in figure 3 where ΔG is the amount in decibels by which the URN-3 antenna gain

Table 2. ILS Localizer C_f Values in Decibels

Desired	Undesired						
	Standard	Directional	Mark I	AN/MRN-7	VOR	AIL 55-E&F	Wilcox 412
Standard	0	-10.5	-0.5	-0.5	1.8	9.0	2.0
Directional	9.5	- 1.0	9.0	9.0	11.4	18.5	11.5
Mark I	-0.5	-11.0	-1.0	-1.0	1.4	8.5	1.5
∞ AN/MRN-7	-0.5	-11.0	0	0	1.4	8.5	1.5
VOR	-1.8	-12.3	-2.3	-2.4	0	7.2	0.2
AIL 55-E&F	-9.0	-19.5	-9.5	-9.5	-7.2	0	-7
Wilcox 412	-2.0	-12.5	-2.5	-2.5	-0.2	7	0

exceeds that of an antenna that just meets specifications. Two curves are shown for the RTA-2 antenna, one for each transmission band (962-1024 MHz and 1151-1213 MHz). These curves were developed using a typical URN-3 radiation pattern (Gierhart and Johnson, 1967, fig. 5). Figure 4 shows the elevation angle at which the direct ray would have to leave the ground facility antenna to arrive at various aircraft positions. This figure can be used to estimate the elevation angle at which ΔG must be considered for a particular aircraft location. Since these angles are not very dependent on the facility antenna height, figure 4 may be used for other navigation aids such as DME, ILS and VOR.

Once the value of ΔG applicable to a particular aircraft location of interest has been determined, it can be used to estimate the maximum¹ EPIRP², E, required for a RTA-2 (isotropic or DME) antenna to provide reliable (95%) service at that location; i. e.,

$$E = E_3 + \Delta G - \Delta G_M \text{ dBW EPIRP}, \quad (2)$$

where E_3 is the EPIRP value required using a URN-3 antenna (fig. 25) and ΔG_M is the amount in decibels by which the main lobe URN-3 antenna gain exceeds that of the antenna type actually used. Values for ΔG_M are as follows:

¹ Gain values greater than those used for the RTA-2 (or DME) antenna in developing fig. 3 would also satisfy the FAA specifications. Therefore, lower ΔG values may be applicable to particular antennas.

² Effective peak isotropic radiated power, EPIRP, is measured relative to an isotropic radiator at the vertical angle of maximum radiation with peak pulse power delivered to the antenna, and is an average over one or more integral number of antenna revolutions. The EPIRP for systems not using pulse techniques (VOR, ILS) is taken as the effective isotropic radiated power (radiated power in dBW plus the main-lobe antenna gain in dB greater than isotropic).

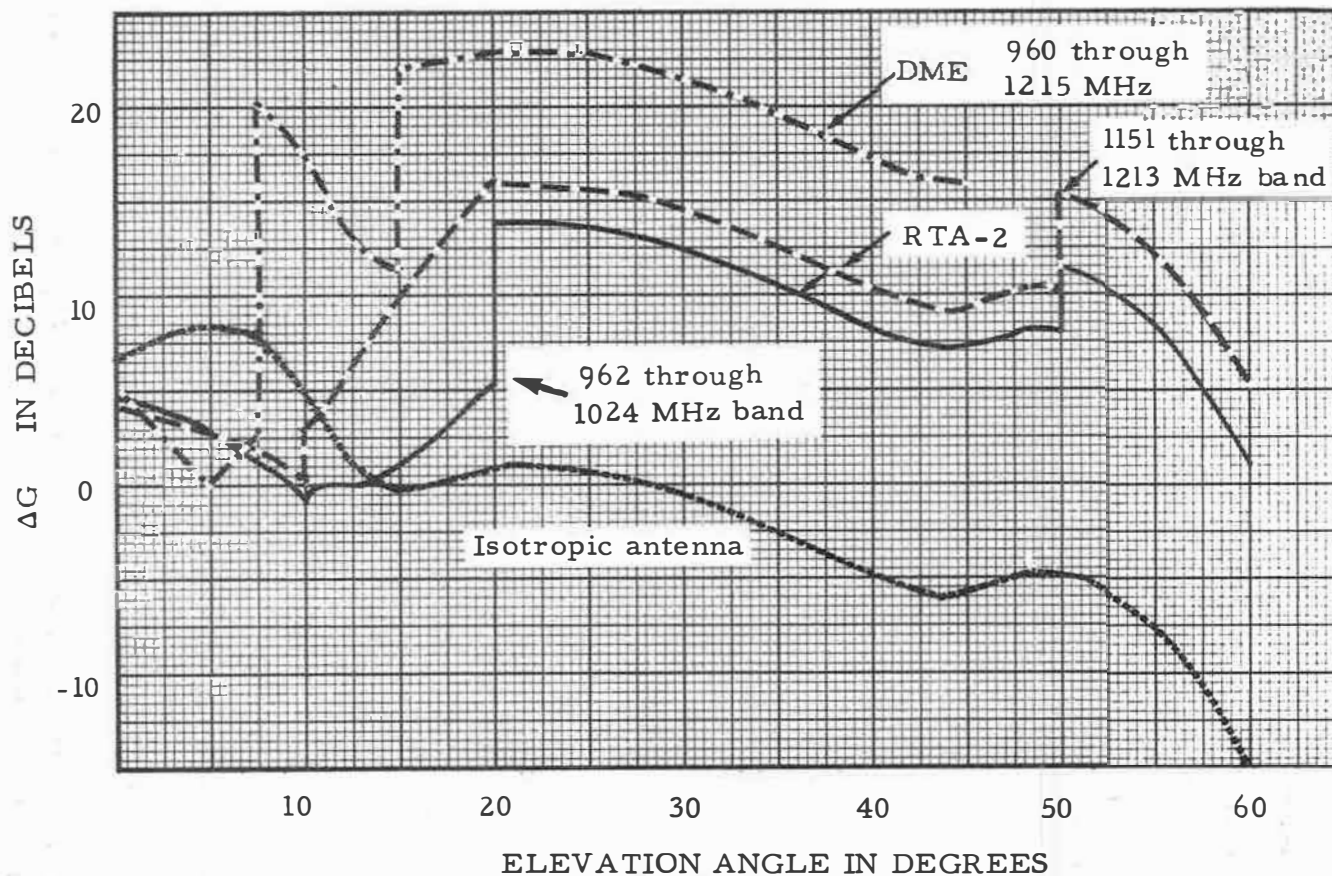


Figure 3. ΔG vs. elevation angle. Relative antenna gain, ΔG is the amount by which the gain of the URN-3 antenna as used by Gierhart and Johnson (1967, fig. 5) exceeds the gain of an isotropic antenna or the minimum gain specified for the RTA-2 antenna (FAA, 1963) or the DME antenna (FAA, 1967).

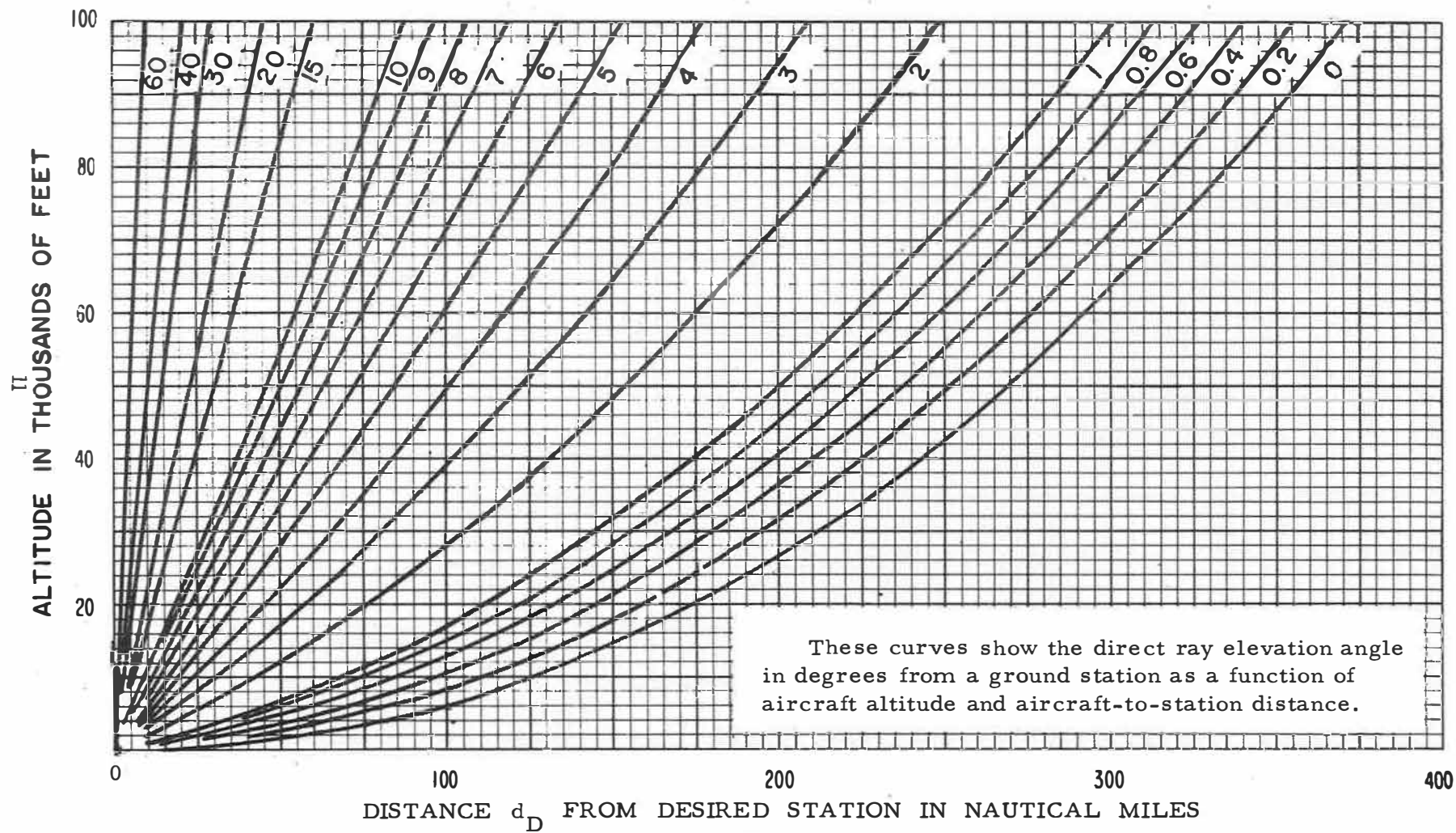


Figure 4. Direct ray elevation angles.

$$G_M = \begin{cases} 1.6 \text{ dB, RTA-2 (962-1024 MHz)} \\ 2.2 \text{ dB, RTA-2 (1151-1213 MHz)} \\ 0.2 \text{ dB, DME} \\ 8.2 \text{ dB, isotropic} \end{cases} \quad (3)$$

Similarly, attenuation, A, greater than free space for a particular location, and RTA-2 (isotropic or DME) antenna can be obtained from

$$A = A_3 + \Delta G \text{ dB} \quad (4)$$

where A_3 is the attenuation value associated with the URN-3 antenna (fig. 15).

For example, since (a) an aircraft located at 144 nm with an altitude of 20,000 ft requires an elevation angle of 0.4° (fig. 4), (b) this angle corresponds to a ΔG of 4.5 dB for a RTA-2 antenna operating in the 962-1024 MHz transmission band (fig. 3), and (c) the value of E_3 that is required for reliable (95%) service at this location is 45 dBW EPIRP (fig. 24), the maximum value of E required for this case as determined from (2) and (3) is approximately 47 dBW EPIRP ($45 + 4.5 - 2.2$). Furthermore, the A_3 for this configuration is 3 dB (fig. 15) so that the maximum A value from (4) is approximately 7.5 dB ($3 + 4.5$).

Some of the curves presented later were calculated using ΔG (figs. 12, 13, 21, 23) and another (fig. 14) was calculated using the RTA-2 antenna pattern shown in figure 5. Gain values greater than those given in figure 5 would also satisfy the FAA specification, and transmission loss calculations made using figure 5 would field values that are too large for such antennas.

GAIN IN DECIBELS GREATER THAN AN ISOTROPIC ANTENNA

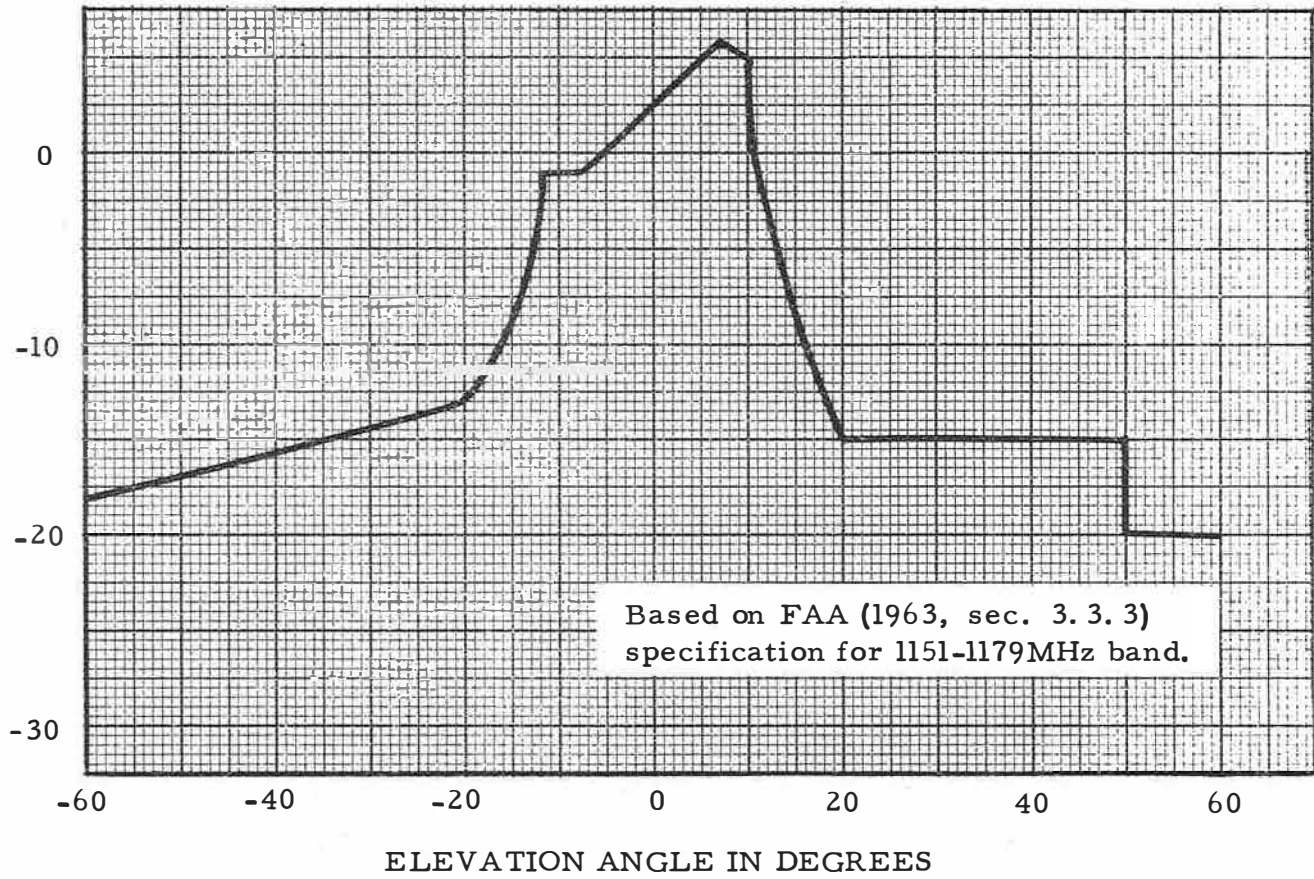


Figure 5. Gain vs. elevation angle; TACAN, RTA-2.

3. PROPAGATION MODELS

The methods used to calculate the curves given in the following sections are based on models for (a) calculated reference transmission loss L_{cr} (b) long-term variability V_{lt} , and (c) short term variability V_{st} . To designate them a set of three codes is used, ($L_{cr} / V_{lt} / V_{st}$); these codes indicate the year that a report for the FAA was first printed with curves developed using the particular model. For example, 62/ 70/No implies that (a) L_{cr} was calculated using the 62 model, (b) long-term variability was calculated using the 70 model, and (c) no short term fading was considered. The list of figures provides the location of curves applicable to various system, antenna, and propagation model combinations. Table 3 summarizes the codes used for propagation model identification. L_{cr} , V_{lt} , and V_{st} models are discussed further in sections 3.1, 3.2, and 3.3, respectively.

3.1 L_{cr} Models

The calculated reference transmission loss, L_{cr} in dB, as used here would be equal to the median transmission loss, $L(50)$ in dB, except for aircraft antenna gain, G_A in dB above isotropic, and a bias, $V(50)$, associated with variability (V_{lt} and/or V_{st}), i. e.,

$$L(50) = L_{cr} - G_A - V(50) \text{ dB} \quad (5)$$

where the gain associated with the ground facility is included in L_{cr} . This section contains more information on the L_{cr} models given in table 3.

Table 3. Propagation Model Codes

Codes	Comments
<u>L_{cr} Models</u>	
62	Models given by Gierhart and Johnson (1962) for TACAN and VOR were used.
62 ΔG	ΔG (fig. 3) was used to revise curves calculated via the 62 L _{cr} model for TACAN with an URN-3 antenna.
69	Median transmission loss values were calculated as in Gierhart and Johnson (1969b) except that (1) antenna gains were considered, (2) a corrective factor similar to the A _Y factor of Gierhart et al. (1970, sec. 3) was used, and (3) atmospheric absorption was neglected.
69 ΔG	ΔG (fig. 3) was used to revise curves calculated via the 69 L _{cr} model for TACAN with an URN-3 antenna.
<u>V_{lt} Models</u>	
62	Models given by Gierhart and Johnson (1962) for TACAN and VOR were used.
65	The long-term variability model associated with Gierhart and Johnson (1965) was used.
70	The long-term variability model recommended by Gierhart et al. (1970, fig. 4) was used.
<u>V_{st} Models</u>	
No	No allowance for short-term fading was included.
67	The variability used for short-term fading was identical with that used by Gierhart and Johnson (1967).
70	The variability used for short-term fading was based on the methods given by Gierhart and Johnson (1967) but with parameters appropriate for particular configurations included.

The 62 L_{cr} models (Gierhart et al., 1962) for TACAN and VOR are described by Gierhart and Johnson (1967, app. I where L_m is used for L_{cr}). TACAN (URN-3 antenna only) and VOR models differ primarily by (a) equipment associated parameters, and (b) the methods used to determine L_{cr} in the line-of-sight region; e.g., diffuse reflection is used with TACAN and specular reflection is used with VOR. Values for L_{cr} were put on computer cards and were used in all calculations involving these models.

The 62 ΔG model utilized the data generated with the 62 L_{cr} model for TACAN (with URN-3) to determine L_{cr} values applicable to DME or TACAN (with RTA-2) by making an adjustment via ΔG (fig. 3). Applicable frequency and facility antenna height are the same as those of the 62 model (1150 MHz and 30 ft).

In the 69 L_{cr} model $L(50)$ values are calculated as in Gierhart and Johnson (1969a, secs. 2 and A.1) except that (a) the antenna gain pattern for the ground facility was considered, (b) a corrective factor similar to the A_Y factor of Gierhart et al. (1970, sec. 3) was used, and (3) atmospheric absorption was neglected.

Initial L_{cr} values, L_{cri} , were obtained using methods developed for (a) forward scatter (Rice et al; 1967, sec. 9), (b) smooth earth diffraction (Rice et al; 1967, sec. 8.1), and (c) line-of-sight (Gierhart and Johnson, sec. A.1). In this line-of-sight method two ray (direct and ground reflected) interference theory (Rice et al; 1967, sec. 5) is used to calculate L_{cri} when the ray path lengths are within a wavelength of each other and the resulting L_{cri} is less than the free-space value L_f ; L_{cri} is set equal to L_f otherwise.

Gierhart et al. (1970, sec. 3) recommends the use of an A_Y factor to prevent available signal powers predicted via the methods of Rice et al. (1967) from exceeding levels expected for free-space propagation by an unrealistic amount, but it is formulated in terms of basic

transmission loss (isotropic antennas) and long-term variability. A more general formulation for A_Y was used in the 69 L_{cr} model, i.e.,

$$A_Y = 0 \text{ dB for } (L_f - 3) < L_{cr} - V(10) \quad (6)$$

otherwise

$$A_Y = L_f + V(10) - L_{cr} - 3 \text{ dB.} \quad (7)$$

The value for $V_{lt}(10)$ is obtained from the V_{lt} models, but is related to L_{cr} by

$$V_{lt}(10) = L_{cr} - L_{lt}(10) \text{ dB} \quad (8)$$

and is positive, since $L_{lt}(10)$ is the transmission loss value that is not exceeded for more than 10% of the hourly-medians.

When the 69 L_{cr} model was used for calculations involving a VOR with an isotropic antenna, the antenna height was taken as 16 ft above ground, and reflections from the counterpoise were neglected. Calculations made using this model for TACAN with a RTA-2 antenna utilize the antenna pattern shown in figure 5.

The 69 ΔG model utilized data generated with the 69 L_{cr} model for a URN-3 antenna pattern to determine L_{cr} values applicable to TACAN (with RTA-2) by making an adjustment via ΔG (fig. 3).

3.2 V_{lt} Models

The curves given in this report as well as those presented by Gierhart et al. (1962), Gierhart (1963, 1964), and Gierhart and Johnson (1965, 1967, 1969a) were developed during a time when the prediction methods given by Rice et al. (1967), Longley and Rice (1968), and Gierhart et al. (1970) were evolving. For convenience,

different V_{lt} models will be identified by the year in which curves developed for the FAA using them were first published. Model year, code (as in table 3), application, source document, and the specific figures developed using it are summarized in table 4. No code is given for the 1969 model since the only curves developed using it for this report are in this section.

Figures 6 and 7 show $V_{lt}(95)$ versus effective distance d_e (Rice et al., 1967, sec. 10.3) for V_{lt} models of table 4. $V_{lt}(95)$ is the amount by which L_{cr} must be decreased to obtain the hourly median transmission loss $L_{lt}(95)$ value that will not be exceeded by 95% of the hourly medians; i. e.,

$$L_{lt}(95) = L_{cr} - V_{lt}(95) \text{ dB.} \quad (9)$$

Curves applicable to ILS localizer and VOR are shown in figure 6. Variability for the ILS glide slope (~ 330 MHz) is not shown, but would be approximately 1.3 times the values shown in figure 6 (Rice et al., 1967, fig. 10.15). Figure 7 is applicable to TACAN.

The $V(p, d)$ function used for V_{lt} in the 1962 models included a function $f(\theta_{et} + \theta_{er})$ that caused excessive dependence on antenna heights; e. g., the difference in the curves shown for aircraft altitudes of 1,000 ft and 100,000 ft on figures 6 and 7. In other V_{lt} formulations, variability for a particular d_e does not vary with antenna height. This $V(p, d)$ was used for all 1962 TACAN calculations, but only for those VOR paths that involved values of angular distance (scattering angle), θ , less than 10 milliradians (mr). Because another function $V(p, \theta)$, similar to $V(p, d)$, was derived primarily from data in the 100 MHz range, the recommendation that it be used when $\theta \geq 10$ mr (Barghausen et al., 1961, ch. 6, sec. IV) was followed in the 1962

Table 4. V_{lt} Models

Year (code), Facility Source Documentation	Figures developed with the model
<p>1962 (62), TACAN Barghausen et al. (1961, ch. 6, sec. IV, V(p, d) for all hours of the year was obtained by averaging V(p, d)'s calculated for summer and winter),</p>	<p>Gierhart et al. (1962, figs. 5, 6, 10-12, 26-38), Gierhart (1963 figs. 5, 14-19), Gierhart (1964, figs. 5, 14-22), Gierhart and Johnson (1967, figs. 9, 28-37, 51-63), this report (figs. 7, 15, 24).</p>
<p>1962 (62), VOR Barghausen et al. (1961), ch. 6, sec. IV, V(p, d) for all hours of the year obtained by averaging V(p, d)'s calculated for summer and winter was used when $\theta < 10$ mr, otherwise V(p, θ) for all hours of year was used),</p>	<p>Gierhart et al. (1962, figs. 5, 7-9, 13-25), Gierhart (1963, figs. 5-12), Gierhart (1964, figs. 5-12), Gierhart and Johnson (1967, figs. 8, 21-27, 38-50), Gierhart and Johnson (1969a, figs. 9, 23-25), this report (figs. 6, 19, 27).</p>
<p>1965 (65), ILS localizer and VOR when used with localizer CCIR (1962, sec. 16.5, V(p, d) for all hours of the year obtained via the analytic functions of sec. 16.6 were used) (a).</p>	<p>Gierhart and Johnson (1965, figs. 5-10), Gierhart and Johnson (1967, figs. 10-20), Gierhart and Johnson (1969a, figs. 10-23, 26-29, this report (fig. 6).</p>
<p>1969 (no code), ILS glide slope Rice et al. (1967, sec. III. 7.1, all hours of the year continental temperate with constants obtained from tables III.5-III.7 was used).</p>	<p>Gierhart and Johnson (1969a, figs. 21, 22), this report figs. 6, 7).</p>
<p>1970 (70), DME, TACAN and VOR Gierhart et al. (1970, fig. 4), Rice et al. (1967, V(50, d) for all hours of the year continental climate via tables III.3 and III.4 was used) (a).</p>	<p>This report (figs. 6, 7, 9-14, 16-18, 20-23).</p>

(a) 1965 and 1970 variabilities about the long-term median are identical except for the frequency factor $g(p, f)$ which differs between CCIR (1962, fig. 70) and Rice et al. (1967, fig. 10.15).

TRANSMISSION LOSS VARIABILITY, $V_{lt}(95)$ IN DECIBELS

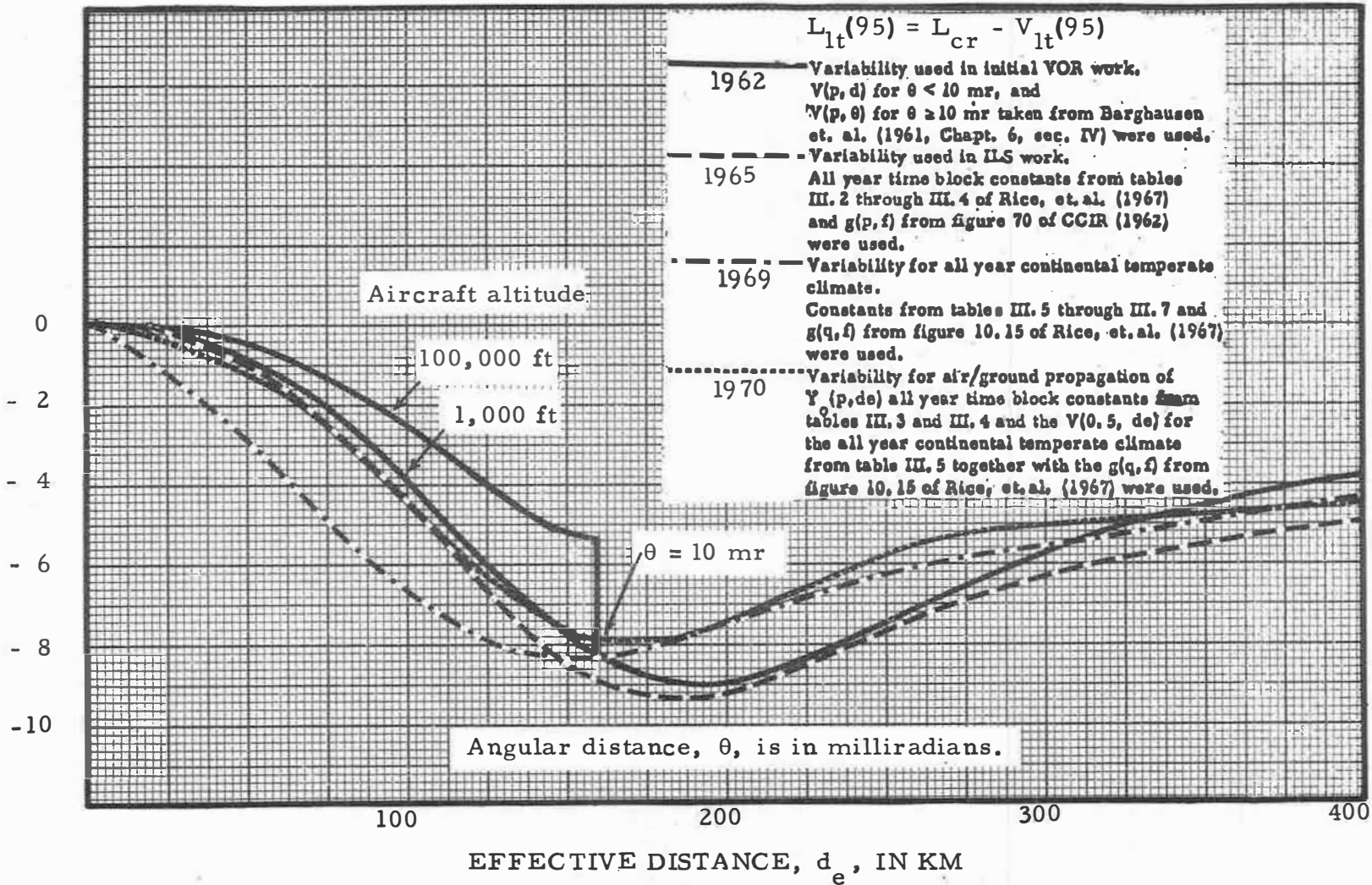
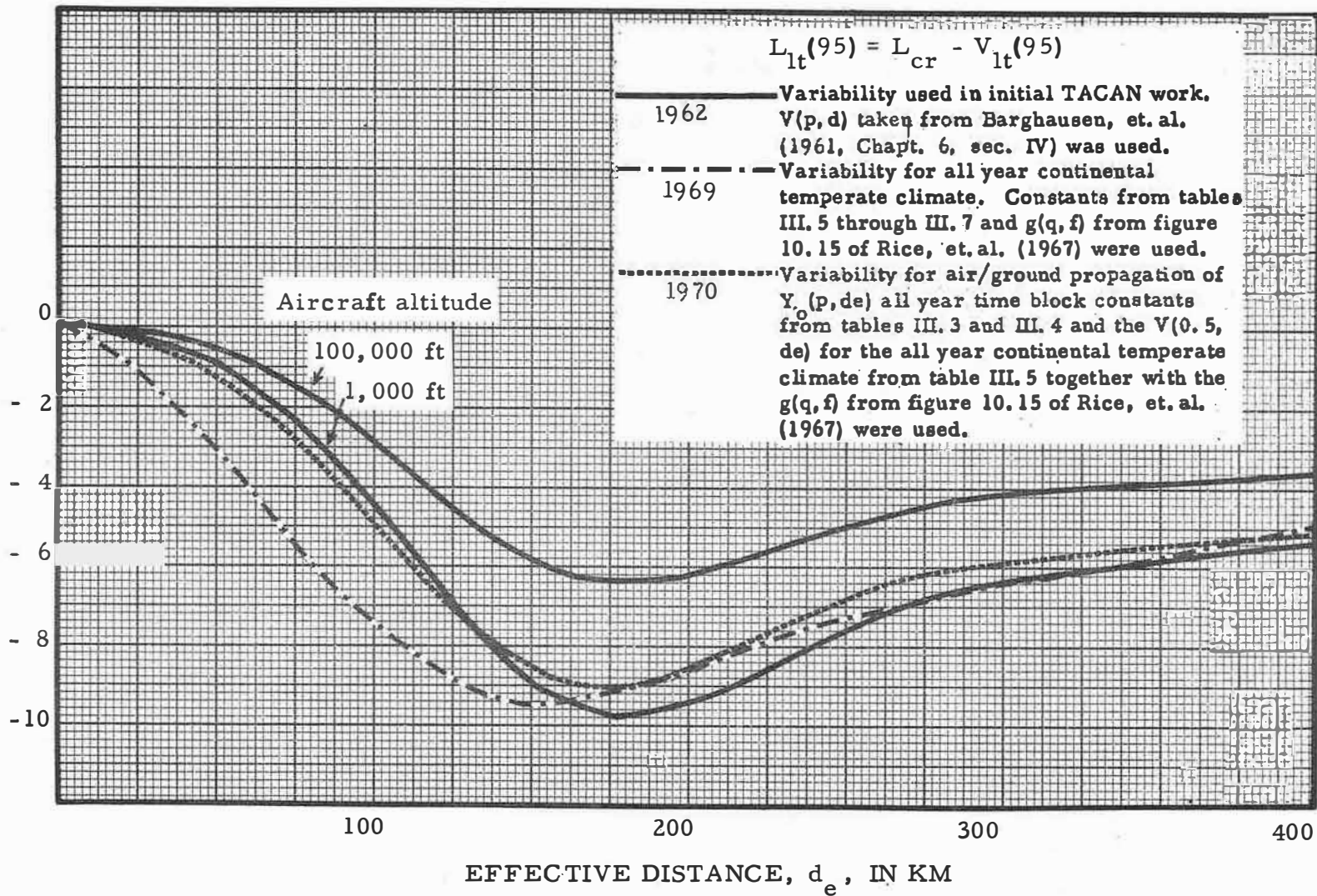


Figure 6. $V_{lt}(95)$ for ILS localizer and VOR.

TRANSMISSION LOSS VARIABILITY, $V_{lt}(95)$ IN DECIBELSFigure 7. $V_{lt}(95)$ for TACAN.

VOR calculations. The transition between $V(p, d)$ and $V(p, A)$ at $\theta = 10$ mrad shown in figure 6 caused abrupt changes in the interference curves as initially calculated for VOR, but these abrupt changes were de-emphasized in the drafting process to obtain smooth continuous curves.

The 1970 model was recommended by Gierhart et al. (1970, fig. 4) after an analysis of air-to-ground propagation data (Barsis et al., 1970) indicated that the variability associated with the continental temperate climate (Rice et al., 1967, tables III.5 to III.7) is too large for line-of-sight air-to-ground paths. This model combines the best features of the all-year continental temperate climate variability model (best estimate of long-term median) and the all-year time block continental temperate climate model (less variability for line-of-sight air-to-ground paths).

3.3 V_{st} Models

Within-the hour variability V_{st} (short-term) of received signal level may be ascribed to phase interference between rays reflected from small layers or scattered from refractive index discontinuities, or to reflections from irregular terrain. Short-term variability could also result from antenna gain variations associated with the moving aircraft. Most of the curves presented in previous reports contain an allowance for these variations. However, curves developed previously for a reference dipole used as the aircraft antenna do not contain such an allowance; i. e., service range without interference information given by Gierhart and Johnson (1967, table 5, figs. 8, 9, nominal range on figs. 21-37; 1969a, table 5, fig. 9, nominal range on fig. 23). All of the prediction curves presented in this report except those of appendix A were developed for reference aircraft antennas (half-wave dipole or isotropic), and the V_{st} models used to develop them do not include aircraft antenna gain variability.

The No V_{st} model is one in which no allowance is made for short-term fading. Only one figure (fig. 9) was developed with short-term fading neglected, and a version of this figure (fig. 10) with short-term fading considered is also given.

The $67 V_{st}$ models are identical with those used by Gierhart and Johnson (1967, app. I) to calculate service range without interference for the ILS localizer, TACAN and VOR. These models are similar to those used previously (Gierhart et al., 1962; Gierhart, 1963, 1964) except that a reference aircraft antenna was assumed and the variability associated with the aircraft antenna $V_A(p, \gamma_{o2})$ was neglected.

The $70 V_{st}$ models are simply an extension of the 67 models using parameter values more appropriate for an isotropic antenna or a RTA-2 TACAN antenna.

The short-term fading formulation used for the isotropic antenna (fig. 10) is the same as the $67 V_{st}$ model except that (a) variabilities associated with reflection from the VOR counterpoise are neglected (Gierhart and Johnson, 1967, sec. I-4, $r = 0$), and (b) the parameter k (Gierhart and Johnson, 1967, eqn. 42) is simply taken as 0.3 since an isotropic antenna is assumed.

The short-term fading formulation used for the RTA-2 TACAN antenna (fig. 14) was extended to other antenna heights by assuming that (a) the VOR counterpoise is not present when the TACAN antenna height above ground is less than 30 ft, and (b) when the counterpoise is present, it is 12 ft above ground and has a diameter of 52 ft; i.e., when the VOR counterpoise is present it is identical with the one used by Gierhart and Johnson (1967, table 2). Based on these assumptions, equations (41) and (43) of Gierhart and Johnson (1967, sec. I.4) were replaced by $|R_C| = 0$ and $R_G = 0.3$, and $V_C'(50, r) - V_F'(50, k)$ in their equation (45) is assumed to be zero when the antenna height, h_1 , above

ground is less than 30 ft. Otherwise ($h_1 \geq 30$ ft) the grazing angle is replaced by ψ_N in equations (41) and (43) mentioned above where

$$\psi_N = \text{Tan}^{-1} \left(\frac{18}{h_1 - 12} \tan \psi \right) \quad (10)$$

and ψ is determined for the particular antenna height of interest using the methods of Gierhart and Johnson (1967, app. I).

4. ILS LOCALIZER STATION SEPARATIONS

Directional ILS localizer antennas usually can be used to reduce the station separation required for a particular desired-to-undesired signal ratio with a 95% reliability, D/U(95). Station separations, S, obtained using figure 14 of Gierhart and Johnson (1967) for a particular case and several configurations are tabulated in table 5. Figures 1 and 2 of Gierhart and Johnson (1967) show antenna gain as a function of azimuth angle α . The median value of desired-to-undesired aircraft antenna gain $R_A(50)$ used by Gierhart and Johnson (1967, fig. 3) is a worst case and is probably too pessimistic when the elevation angle of the direct-ray from the desired station to the aircraft, γ_{o2} , is $\sim 0^\circ$ (Gierhart and Johnson, 1967, fig. 4). A value of $R_A(50) = 0$ dB could probably be used with the Gierhart and Johnson (1967) curves with little danger of underestimating potential interference, and table 5 also gives the separations resulting from such a procedure; i. e., increasing normalized D/U, $N\{D/U(95)\}$, of Gierhart and Johnson (1967, sec. 5.2) by 3 dB to obtain values applicable for $R_A(50) = 0$ dB.

The maximum station separation reduction shown in table 5 for use of a directional instead of a standard antenna is 32 nm or 28% of 115 nm

Table 5. ILS Localizer Station Separations

Desired/undesired	$\alpha^{(a)}$ deg	N {D/U(95)} dB	$S^{(b)}$ nm	$S^{(c)}$ nm
Standard/standard	0	20	124	122
Directional/dir- ectional	0	21	125	123
Standard/standard	90	15	119	115
Directional/dir- ectional	90	3.5	93	83

(a) The angle between the main-lobe azimuth of the undesired localizer carrier antenna and the azimuth of the aircraft from the undesired station is α (see fig. 1).

(b) Values from fig. 14 of Gierhart and Johnson (1967) for $D/U(95) = 20$ dB, aircraft altitude of 6, 250 ft and a desired distance of 25 nm.

(c) Values for a N {D/U(95)} decrease of 3 dB to consider $R_A(50) = 0$ dB case.

($S^{(c)}$ for $\alpha = 90^\circ$). This may seem small in view of the 12 dB difference in N {D/U(95)}, but figure 8 shows that L_{cr} for the undesired ILS localizer is increasing at a rate of 0.4 dB/nm at 70 nm and at a rate of 1.1 dB/nm at 100 nm.

Curves given by Gierhart and Johnson (1967) indicate that D/U(95) values available with VOR's may be significantly greater than those available for ILS localizers for similar station configurations. For example, D/U(95) is ~17 dB, for VOR (Gierhart and Johnson, 1967, fig. 22) and ~2 dB for ILS (Gierhart and Johnson, 1967, fig. 14) when a desired station distance of 25 nm, an aircraft altitude of 6, 250 ft and a station separation of 90 nm are assumed. About 10 dB of this 15 dB difference comes from the difference in the L_{cr} curves used for the two facilities (fig. 8), about 3 dB is associated with the $R_A(50) = -3$ dB used for ILS and the remaining ~2 dB is probably due to a difference in the variability models used.

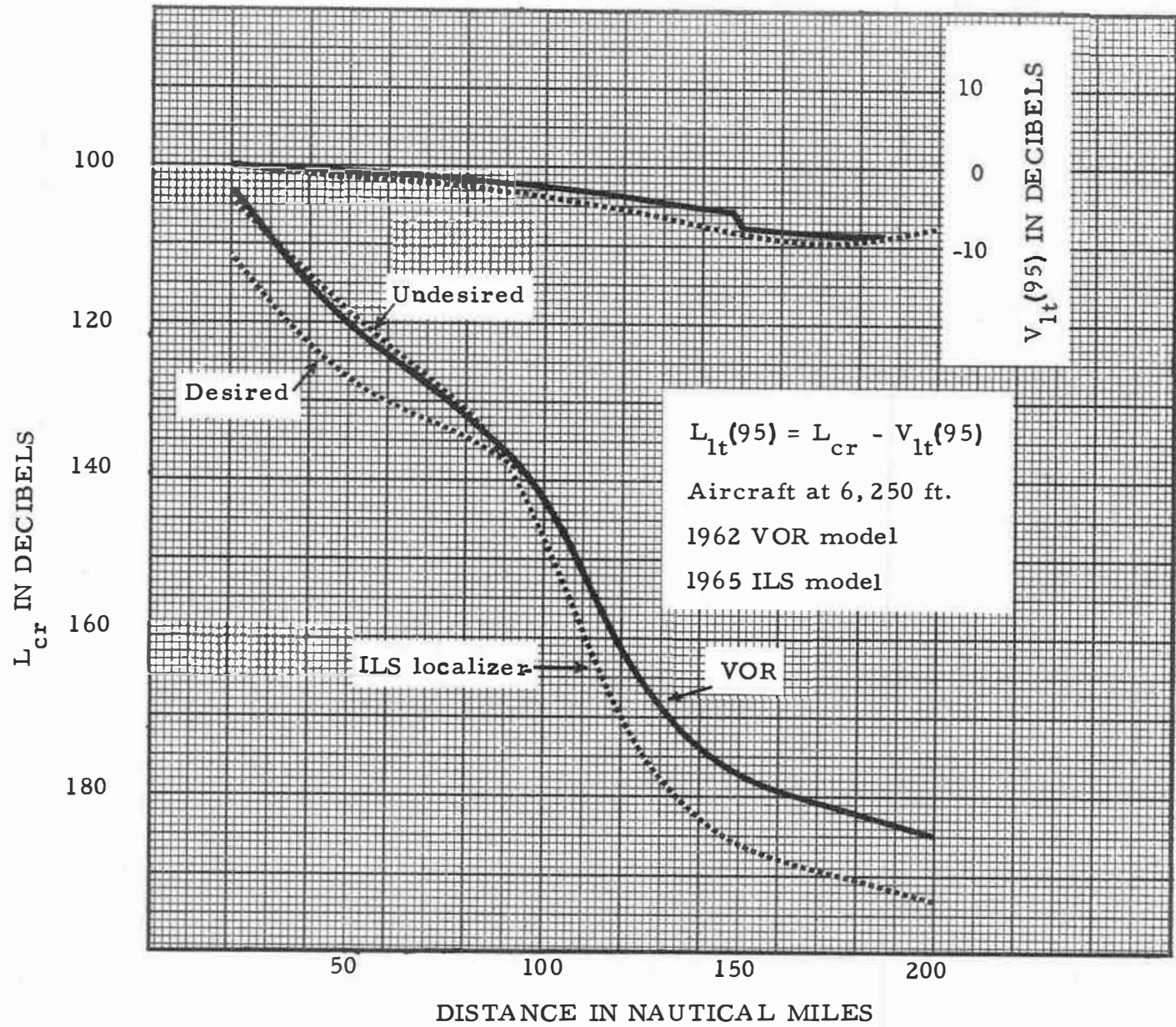


Figure 8. L_{cr} and $V_{lt}(95)$ vs. distance; ILS localizer and VOR.

A $N\{D/U(95)\}$ of ~ 12 dB would be obtained for ILS if (a) $R_A(50) = 0$ dB, and (b) the L_{cr} curve for desired ILS were used for both desired and undesired ILS stations. About 3 dB of the remaining VOR advantage in this case can be attributed to the higher antenna height used for VOR (16 ft as compared to 5.5 ft for ILS).

VOR and ILS would have $D/U(95)$'s of ~ 5 and ~ 7 dB respectively when (a) $R_A(50) = 0$ dB is used for ILS, and (b) the Longley and Rice (1968) model with the A_Y correction recommended by Gierhart et al. (1970, sec. 3) is used in L_{cr} calculations. These small $D/U(95)$'s occur because use of the Longley and Rice (1968) model yields free space loss values for both VOR and ILS at distances less than ~ 60 nm when the aircraft is at 6,250 ft. Indiscriminate application of the Longley and Rice (1968) model to the prediction of potential interference for air navigation aids is probably not justified even when the conditions for which the model is applicable are met (Longley and Rice, 1968, sec. 1).

5. ATTENUATION CURVES

Curves of attenuation greater than free space basic transmission loss, L_{bf} , versus distance are shown in figures 9 through 20 which are located at the end of this section. Each figure indicates the system and ground antenna type to which the figure is applicable along with the model used to develop it. The list of figures provides a useful guide to the curves available. All of these curves are applicable to the special case where the aircraft antenna is isotropic and the reliability or time availability is 95%; i. e., attenuation values less than those shown would be expected 95% of the time.

For convenience, L_{bf} values based on great-circle path distance instead of ray-path length were used to convert transmission loss, L_{IA} , obtained from the models discussed in section 3 to attenuation,

i. e.,

$$A = L_{IA} - L_{bf} \text{ dB} \quad (11)$$

and

$$L_{bf} = 37.8 + 20 \log_{10} f_{\text{MHz}} + 20 \log_{10} d_{\text{nm}} \text{ dB} \quad (12a)$$

where f_{MHz} is frequency in megahertz and d_{nm} is great-circle path distance in nautical miles. For the frequencies used in this report

(12a) becomes

$$L_{bf} = 78.9 + 20 \log_{10} d_{\text{nm}} \text{ dB at 113 MHz,} \quad (12b)$$

$$L_{bf} = 79.2 + 20 \log_{10} d_{\text{nm}} \text{ dB at 118 MHz,} \quad (12c)$$

$$L_{bf} = 99.0 + 20 \log_{10} d_{\text{nm}} \text{ dB at 1150 MHz,} \quad (12d)$$

or

$$L_{bf} = 99.4 + 20 \log_{10} d_{\text{nm}} \text{ dB at 1200 MHz.} \quad (12e)$$

This procedure allows L_{IA} to be recovered from

$$L_{IA} = L_{bf} + A \text{ dB} \quad (13)$$

where the determination of L_{bf} requires only the path distance used as an abscissa on the figures. For example,

$$L_{IA} = 142.9 + 16 = 158.9 \text{ dB}$$

when A is determined from figure 11 for an aircraft altitude of 14,500 ft and a d_{nm} of 150 nm, and 142.9 is the L_{bf} value calculated from (12e), i. e.,

$$L_{bf} = 99.4 + 43.5 = 142.9 \text{ dB.}$$

Ray length and path distance are nearly equal in most applications, but in cases where the magnitude of aircraft altitude is about equal or greater than the magnitude of the path distance it is possible for the ray length to be significantly greater than the path distance. In such cases, the A values will increase with decreasing distance, e.g., see figure 10 for $d_{nm} < 15$ nm.

Figure 9 is the only figure that was developed without consideration of short-term fading. This is why $A = 0$ was obtained even though antenna directivity was not available to discriminate against diffuse ground reflection. Figure 10, which was developed for similar conditions but with short-term fading considered, indicates that the short-term fading associated with diffuse reflection would prevent A from becoming less than about 4 dB. Note that the VOR model does not include an allowance for diffuse reflection and low values of A are possible even with an isotropic antenna; e.g., see figure 18 for $d_{nm} < 15$ nm.

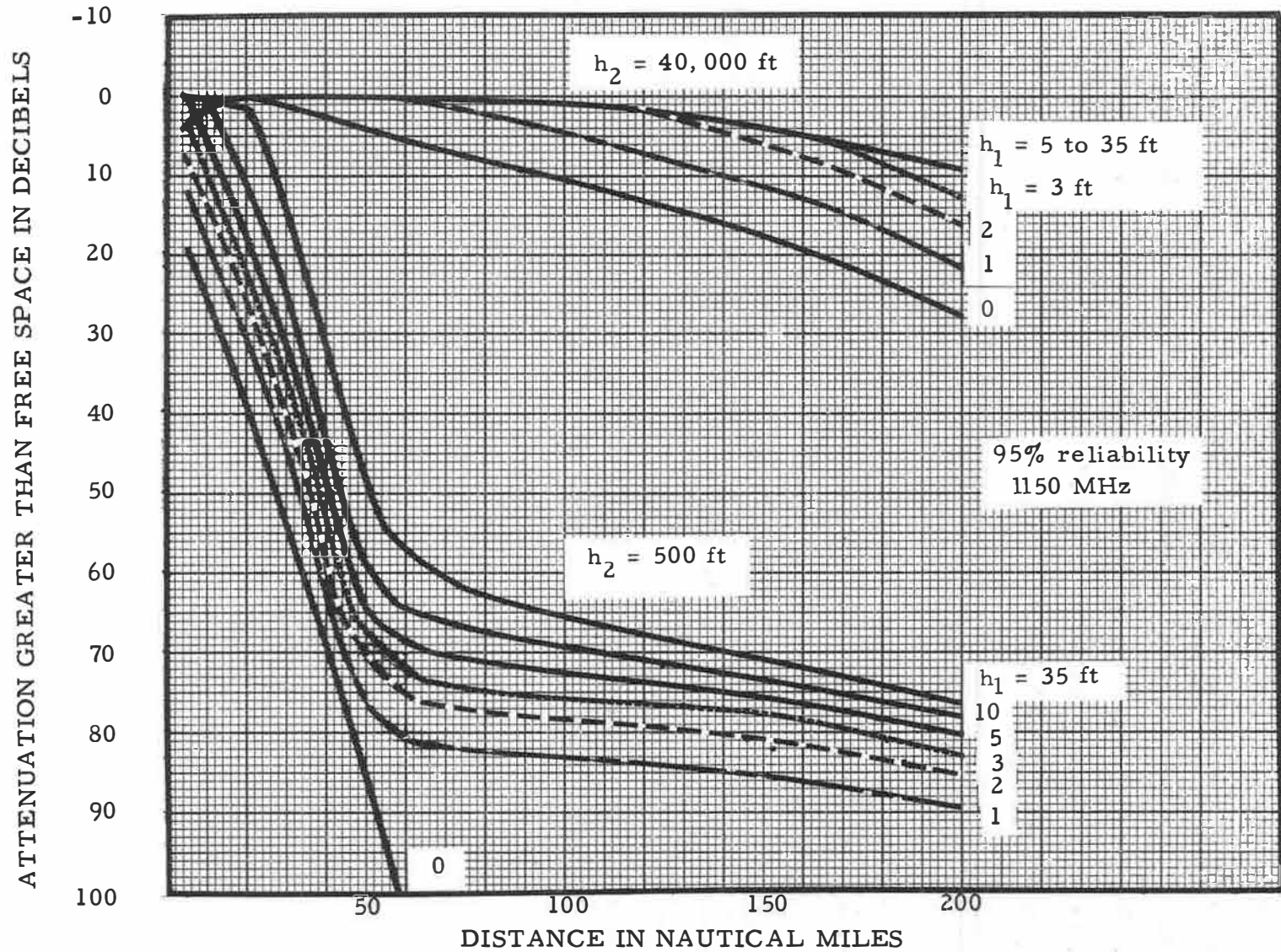


Figure 9. Attenuation greater than free space vs. distance; 1150 MHz, isotropic antenna, 69/70/No, $h_1 = 0 \text{ to } 35 \text{ ft}$.

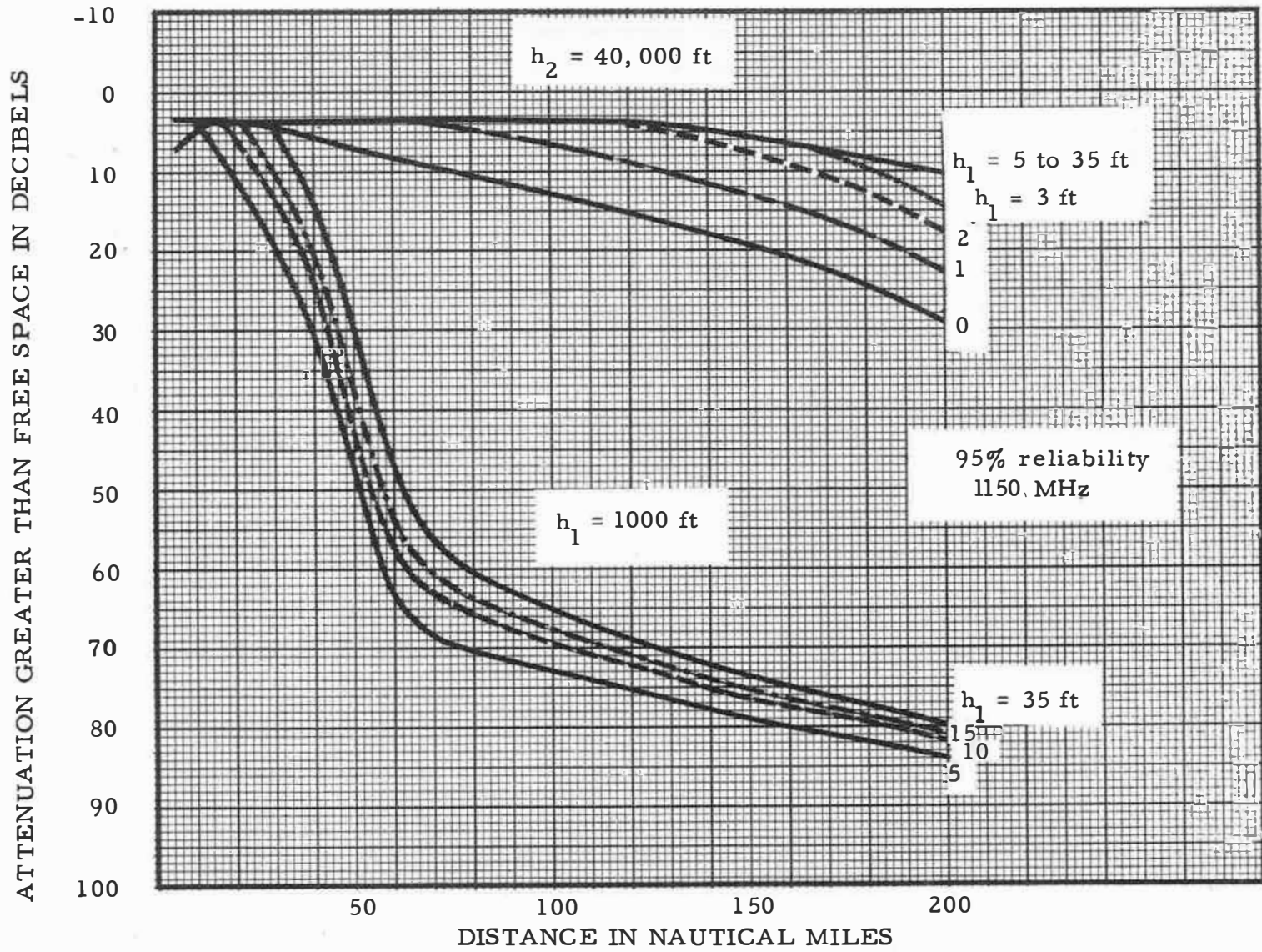


Figure 10. Attenuation greater than free space vs. distance; 1150 MHz, isotropic antenna, 69/70/70, $h_1 = 0$ to 35 ft.

FREQUENCY 1200 MHz

RELIABILITY 95%

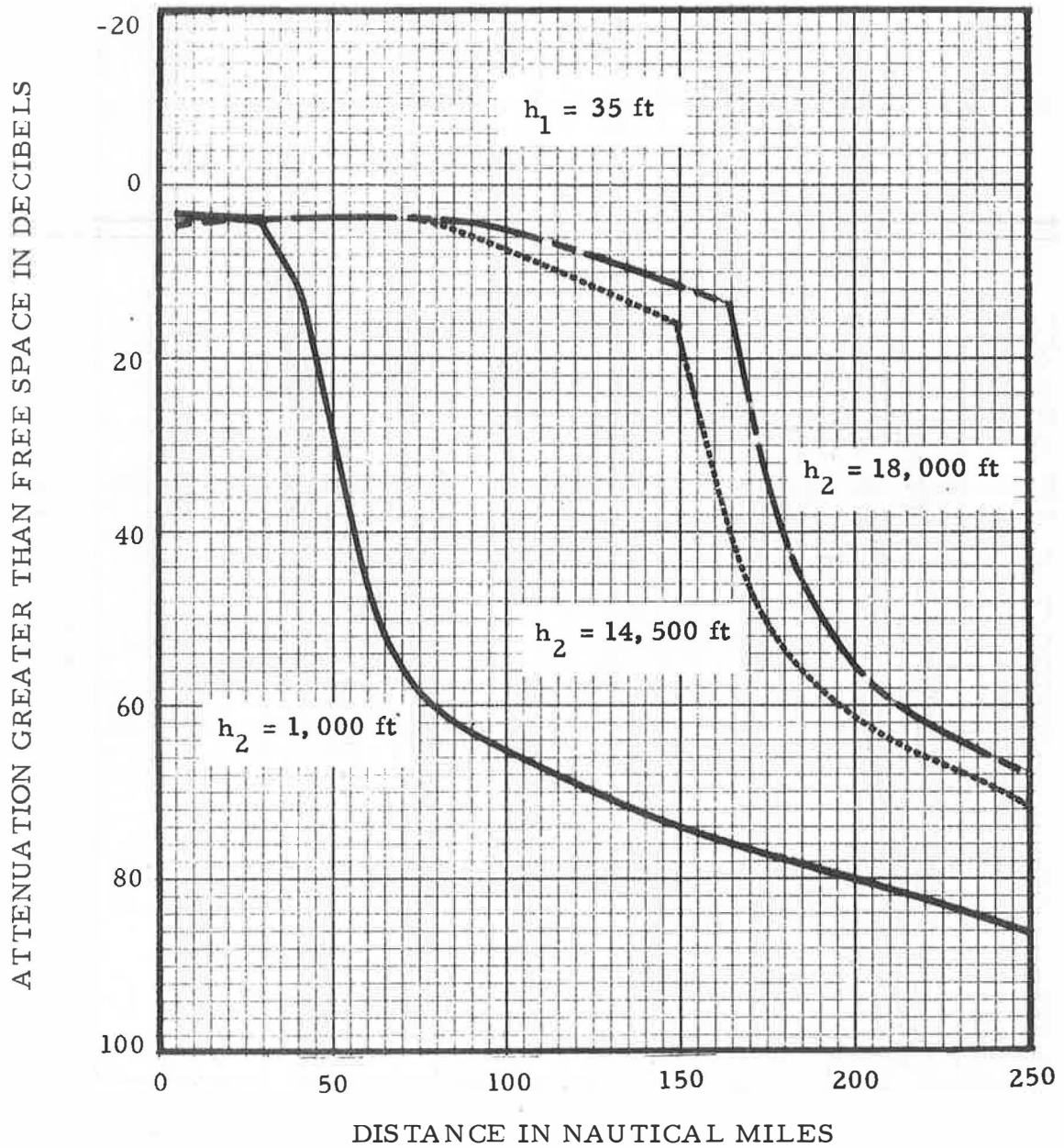


Figure 11. Attenuation greater than free space vs. distance; 1200 MHz, isotropic antenna, 69/70/70.

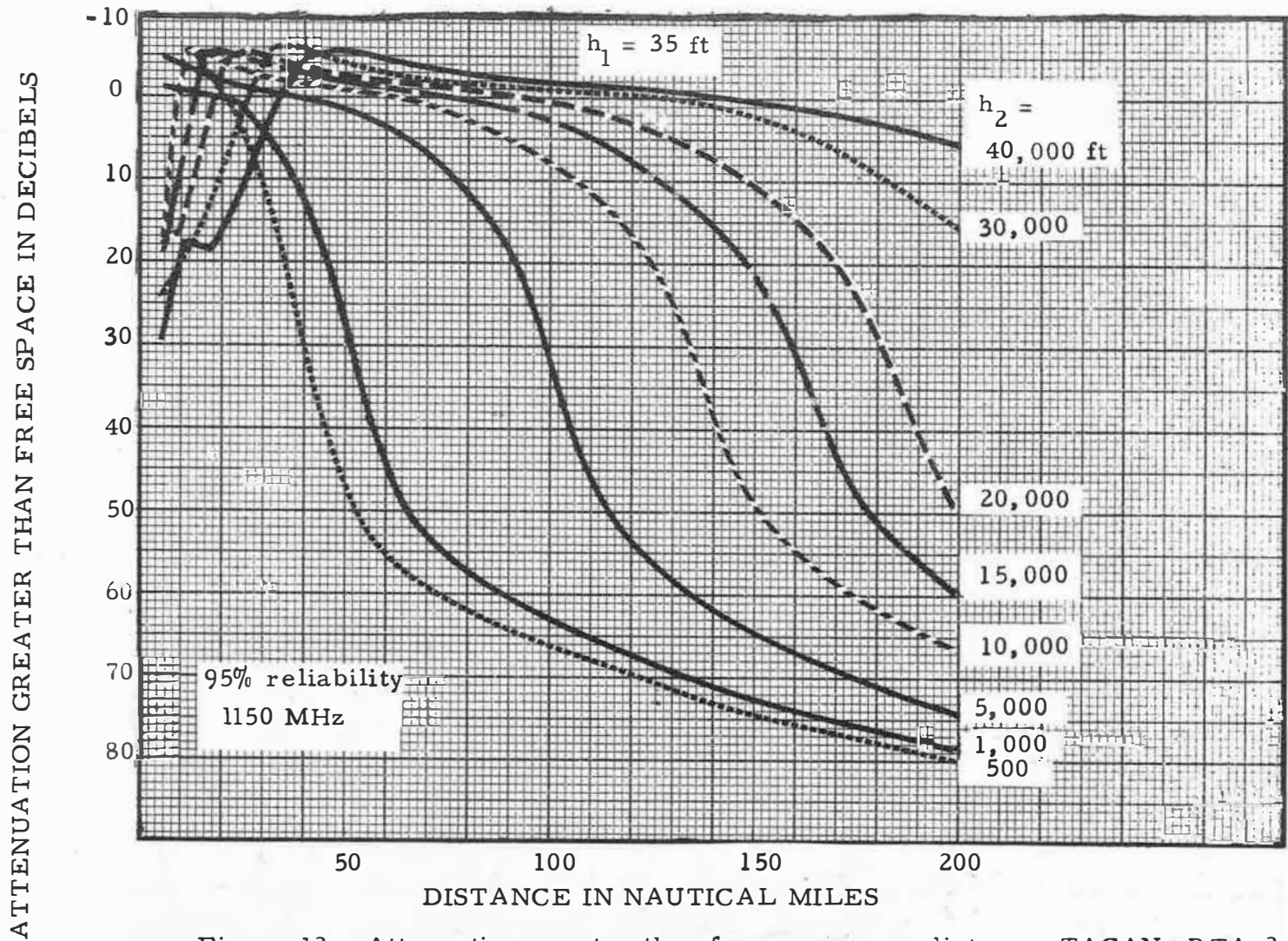


Figure 12. Attenuation greater than free space vs. distance; TACAN, RTA-2, 62ΔG/70/67.

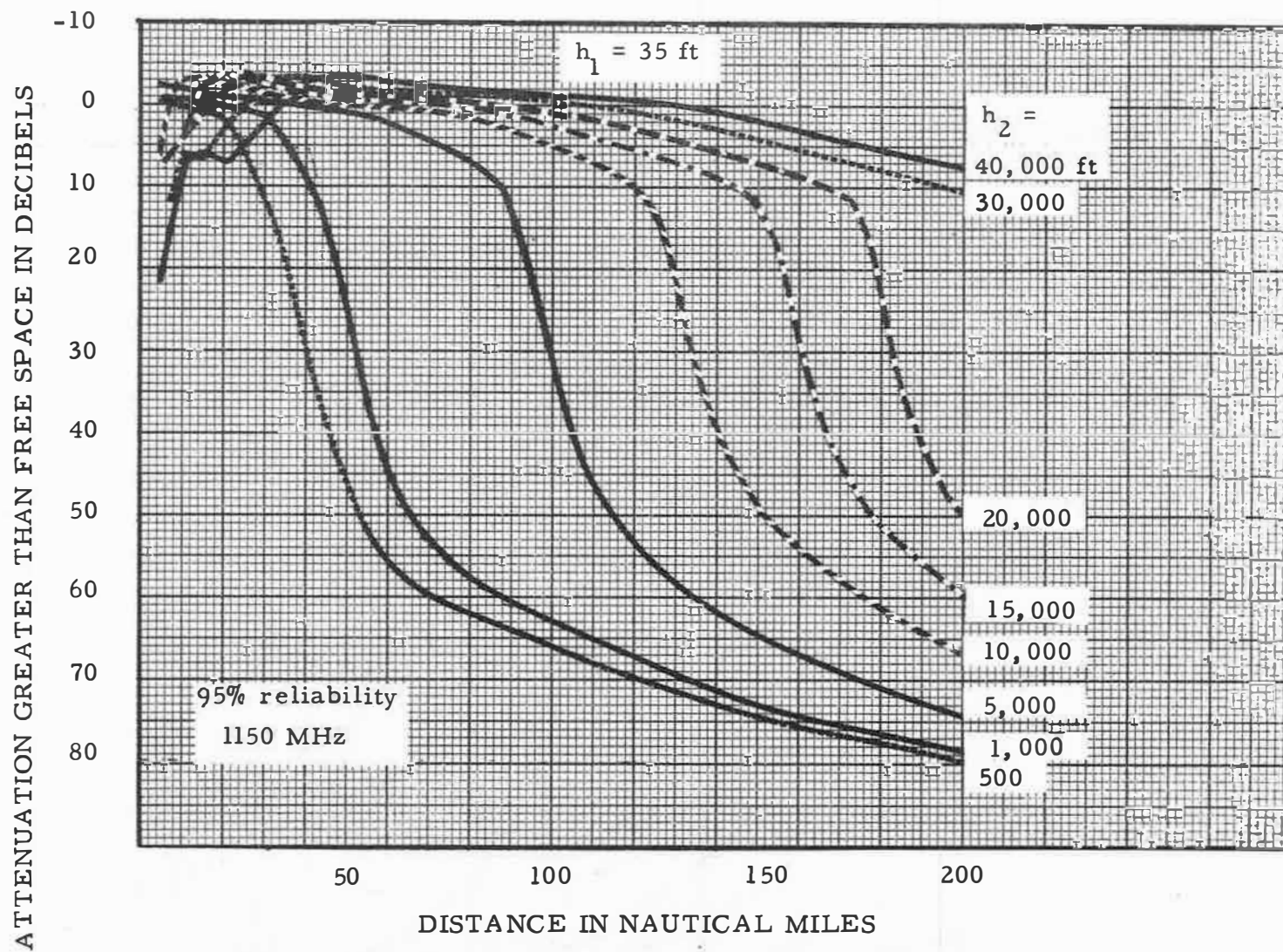


Figure 13. Attenuation greater than free space vs. distance; TACAN, RTA-2, 69 ΔG/70/67.

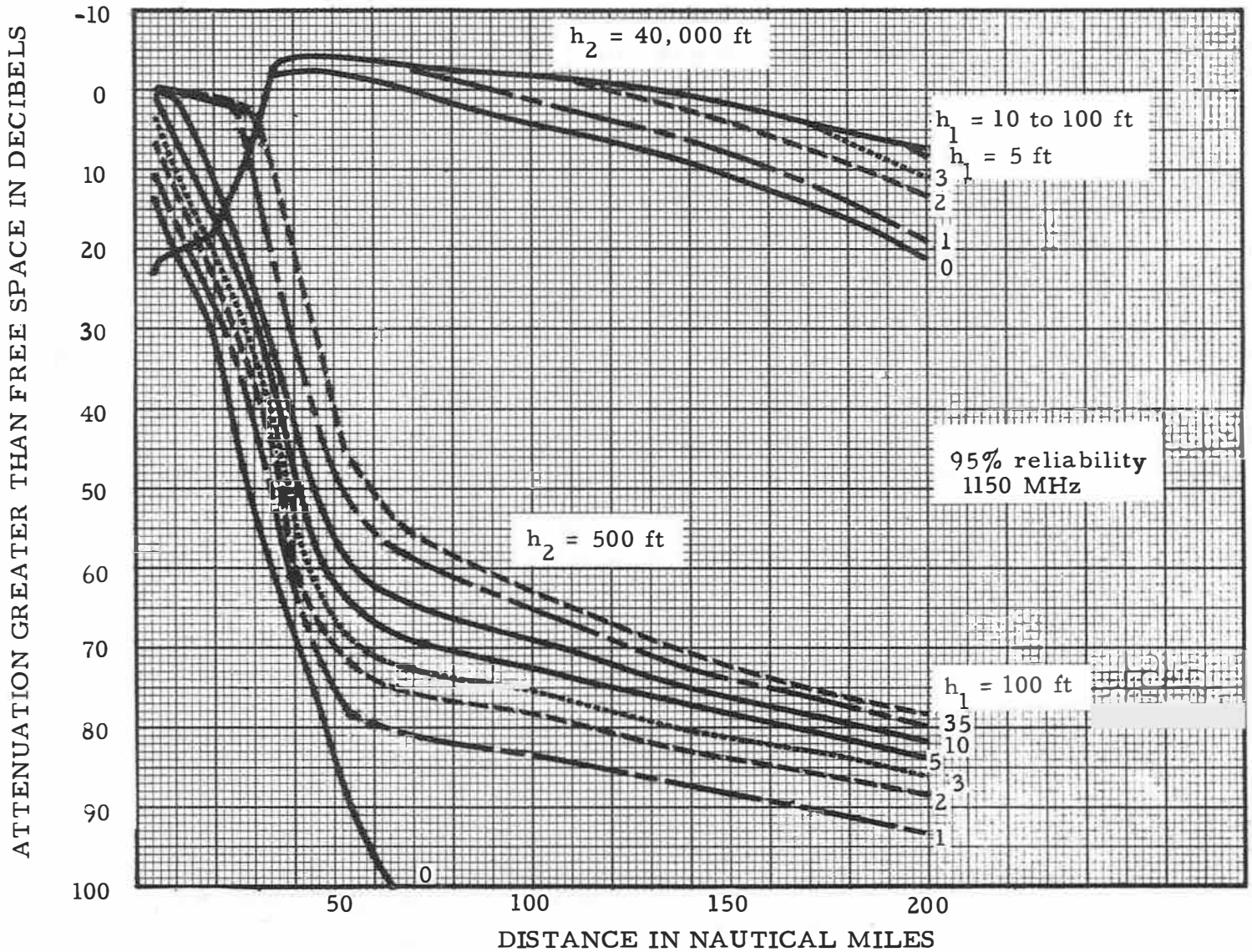


Figure 14. Attenuation greater than free space vs. distance; TACAN, RTA-2, 69/70/70, $h_1 = 0 \text{ to } 100 \text{ ft.}$

ATTENUATION GREATER THAN FREE SPACE IN DECIBELS

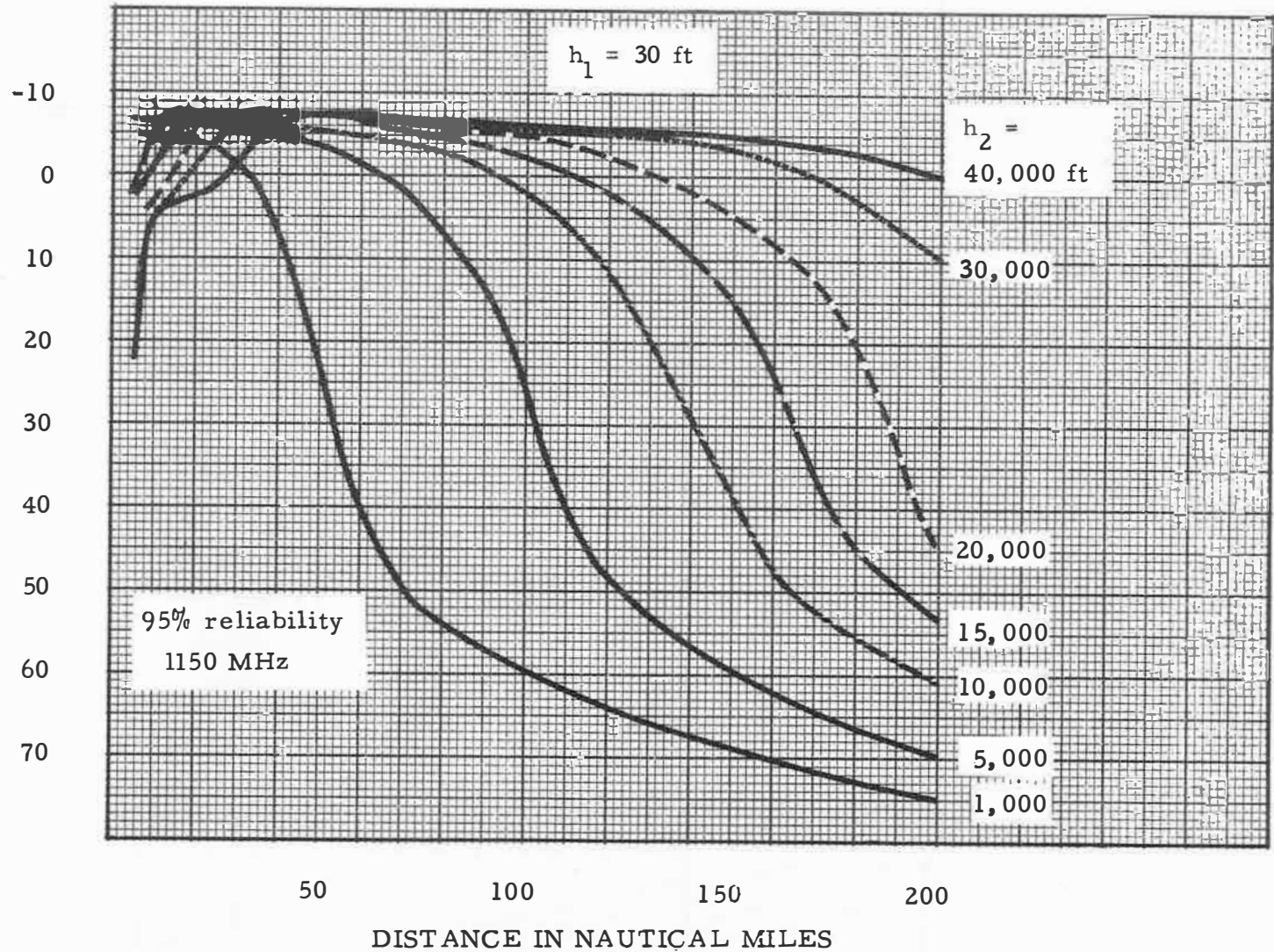


Figure 15. Attenuation greater than free space vs. distance; TACAN, URN-3, 62/62/67.

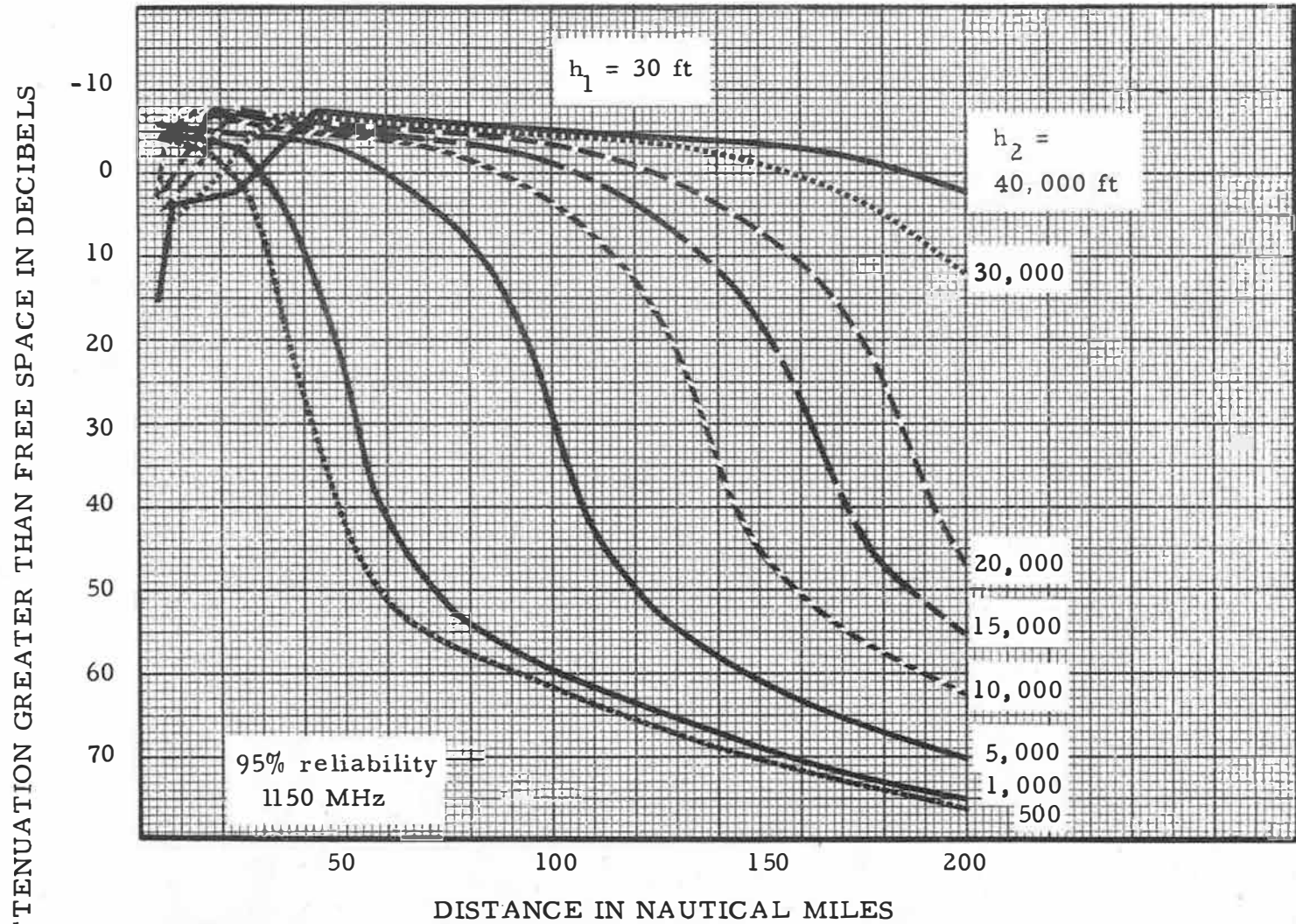


Figure 16. Attenuation greater than free space vs. distance; TACAN, URN-3, 62/70/67.

ATTENUATION GREATER THAN FREE SPACE IN DECIBELS

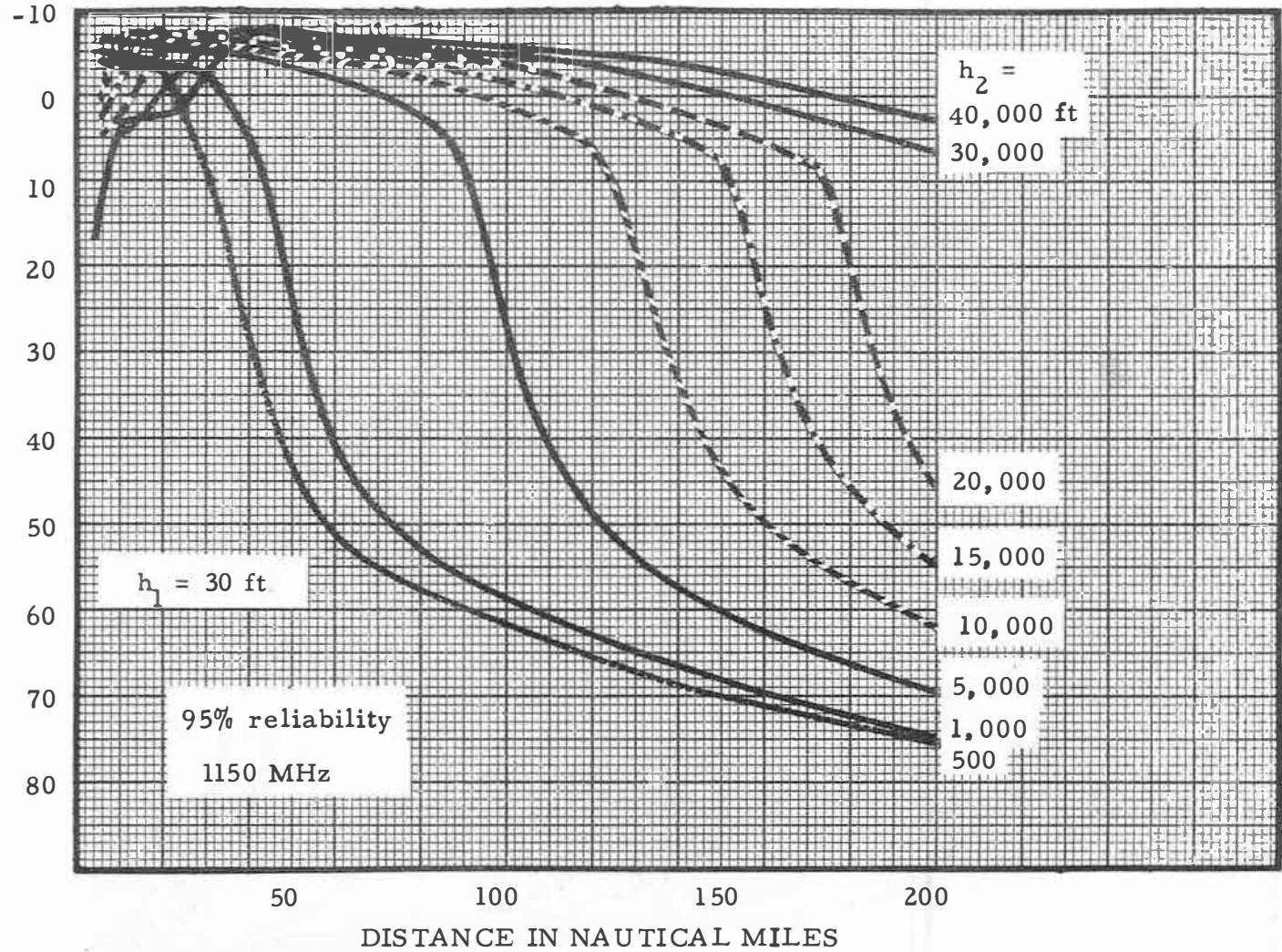


Figure 17. Attenuation greater than free space vs. distance; TACAN, URN-3, 69/70/67.

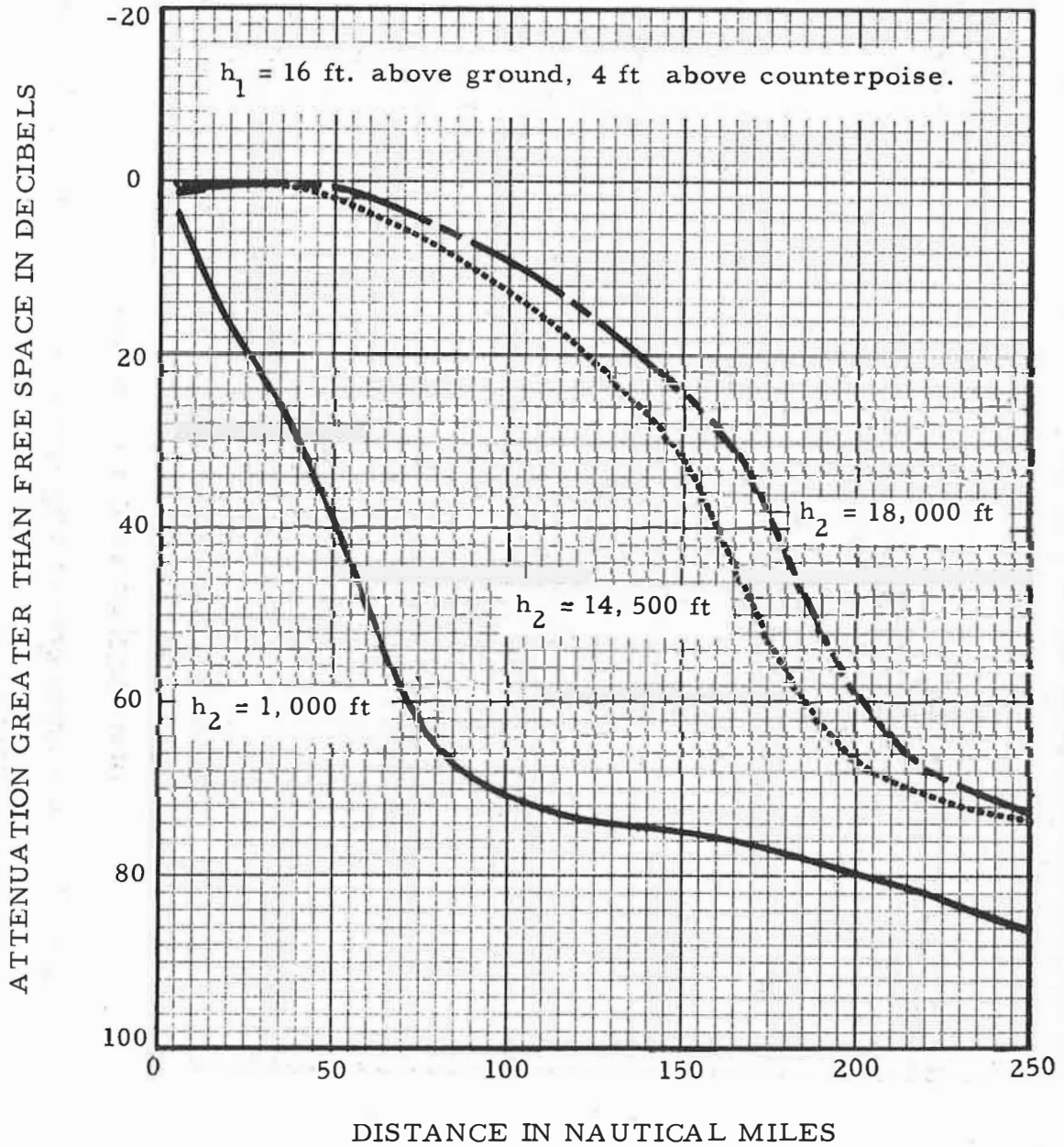


Figure 18. Attenuation greater than free space vs. distance; 118 MHz, isotropic antenna, 69/70/67.

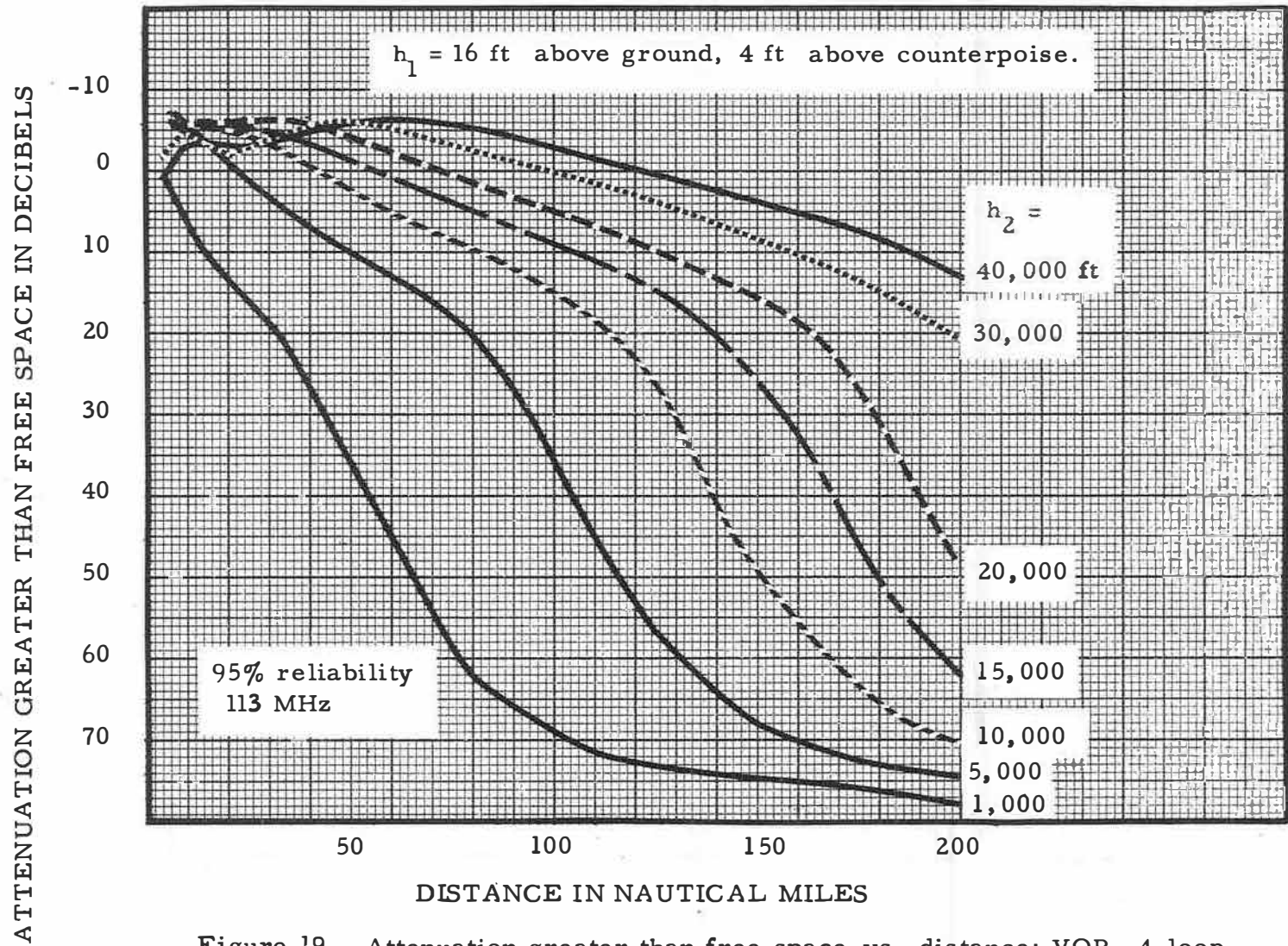


Figure 19. Attenuation greater than free space vs. distance; VOR, 4-loop, 62/62/67.

ATTENUATION GREATER THAN FREE SPACE IN DECIBELS

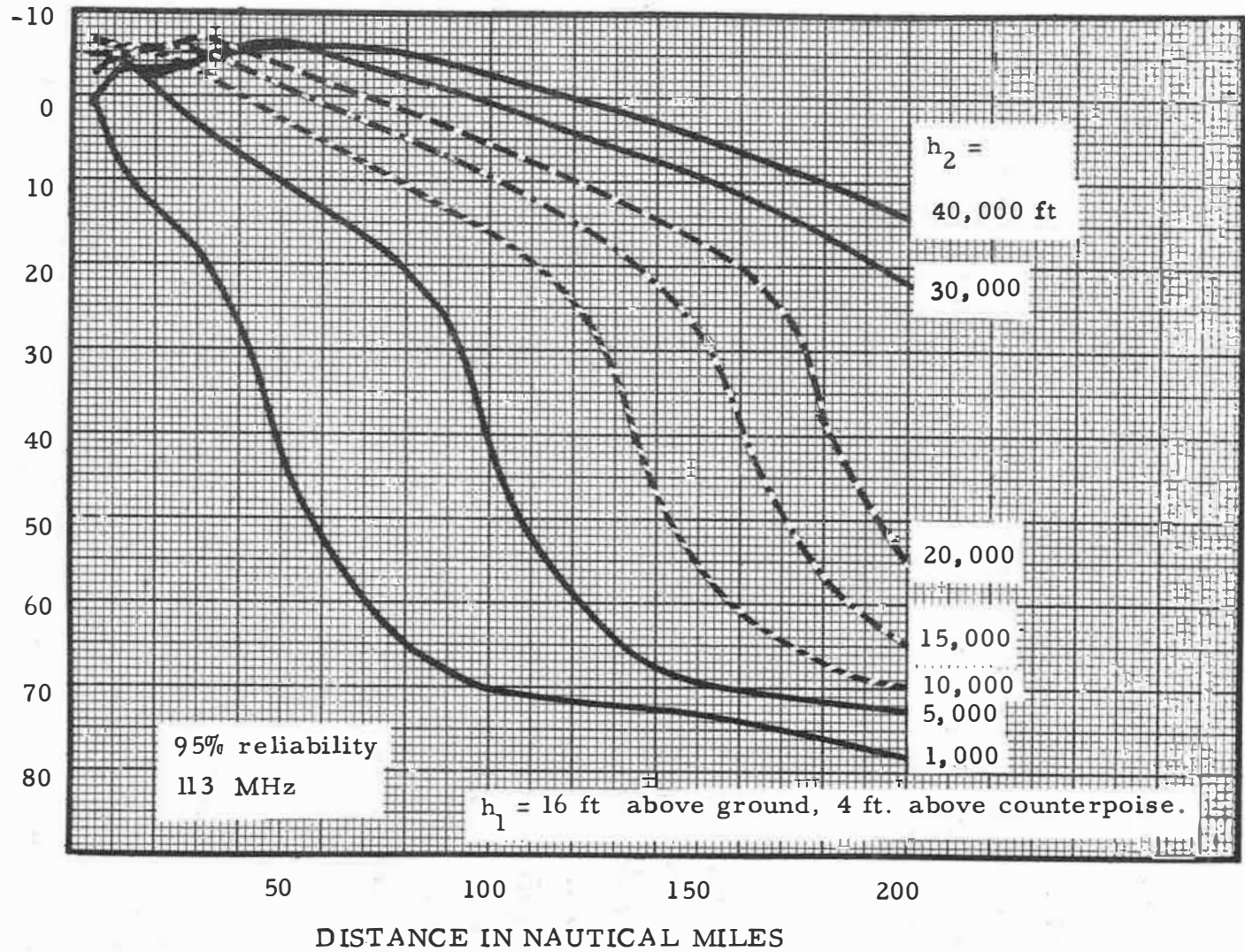


Figure 20. Attenuation greater than free space vs. distance; VOR, 4-loop, 62/70/67.

6. SERVICE VOLUME CURVES

Service volume without interference curves similar to those given by Gierhart and Johnson (1967, sec. 5.1) are shown in figures 21 through 27 at the end of this section. Each figure indicates the system and antenna type to which the figure is applicable along with the model used to develop it. The list of figures provides a useful guide to the curves available. All of these curves are applicable to the special cases where the aircraft antenna is either a reference dipole or isotropic and the reliability or time availability is 95%; i. e., the rotation of a particular curve about its ordinate axis defines a volume in which the radiated power implied by the curve is sufficient to produce the required available power at the receiving antenna at least 95% of the time.

Power available at the terminals of a reference dipole (half-wave) is used to define satisfactory service in figures 21, 23, 24, 25 and 27. Vertical polarization was used for DME and TACAN, and horizontal polarization was used for VOR. Figure 22 for DME and figure 26 for VOR have satisfactory service defined in terms of the power available at the terminals of an isotropic antenna. Table 6 gives the reference

Table 6. Reference Power Equivalents

Reference power in dBW for half-wave dipole	-112 ^(a)	-112	-106 ^(a)	-107	-122
for isotropic antenna	-114	-114 ^(a)	-108	-109 ^(a)	-124 ^(a)
Frequency in MHz	113	118	1150	1200	1200
Power density in dBW/m ²	-112	-111	-86	-86	-101

^(a) Values actually used on figures.

power equivalent for the various power levels used to define satisfactory service in terms of both reference antenna types and power density. Power densities were calculated by subtracting $10 \log_{10}$ of the effective area for a reference antenna from the reference power (in dBW) associated with it (Gierhart and Johnson, 1967, sec. 5.1).

Figure 22 shows service volume without interference curves for a DME facility with an isotropic antenna. These curves show the effective peak isotropic radiated power EPIRP (see footnote 2 of sec. 2.2) required for the ground-to-air link when -109 dBW or greater must be available at the terminals of an airborne isotropic antenna with a 95% reliability. Each of these curves has an additional EPIRP value shown in parentheses; these are EPIRP's required for the air-to-ground link when -124 dBW or greater must be available at the terminals of an isotropic ground facility antenna.

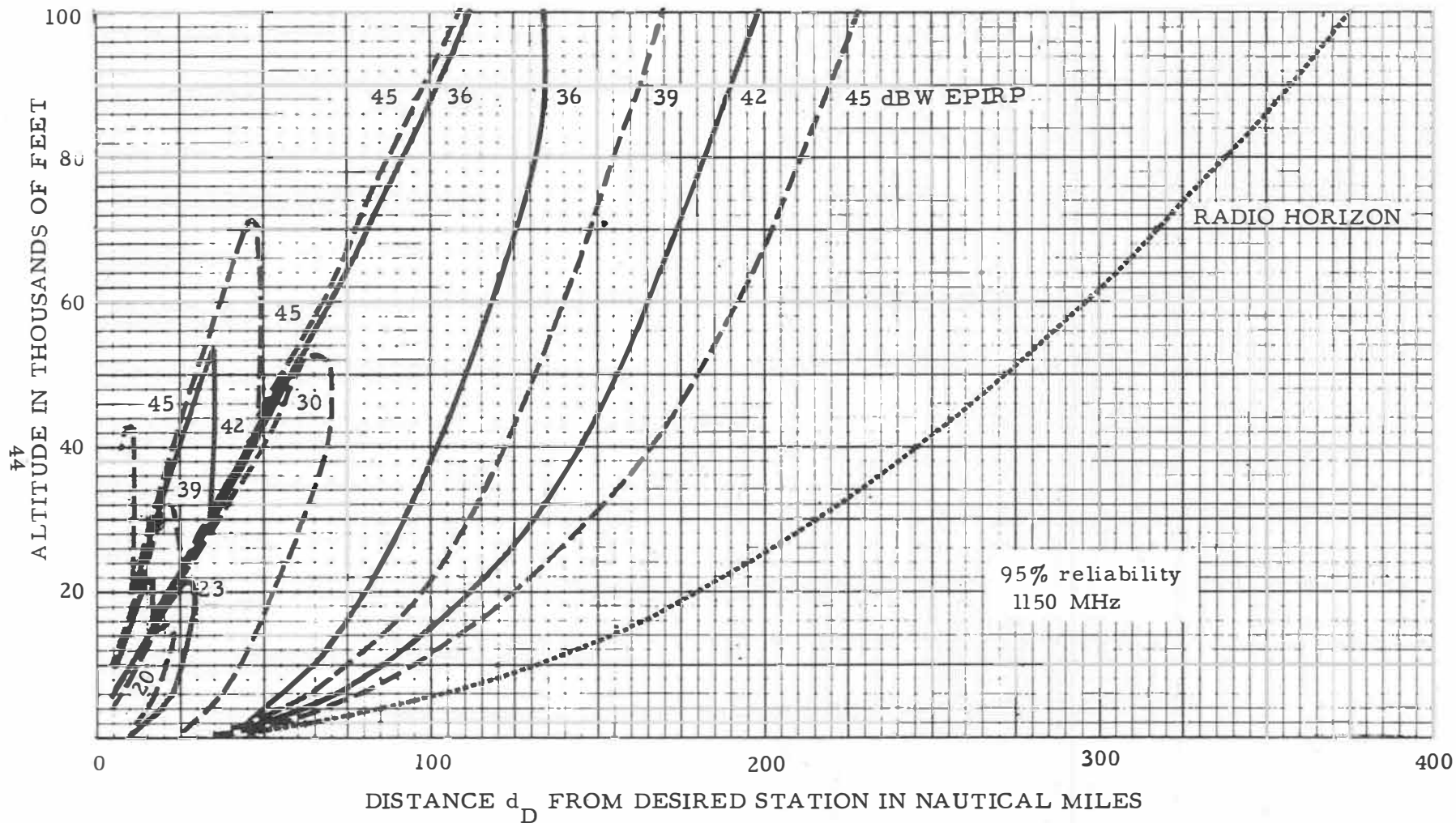


Figure 21. Service volumes without interference; DME antenna, $62 \Delta G/70/67$. The reference power of -106 dBW is equivalent to a power density of -86 dBW/m². The effective peak isotropic radiated power (EPIRP) required to produce -106 dBW of available power from a reference half-wave dipole located on the service volume boundary is given for each curve.

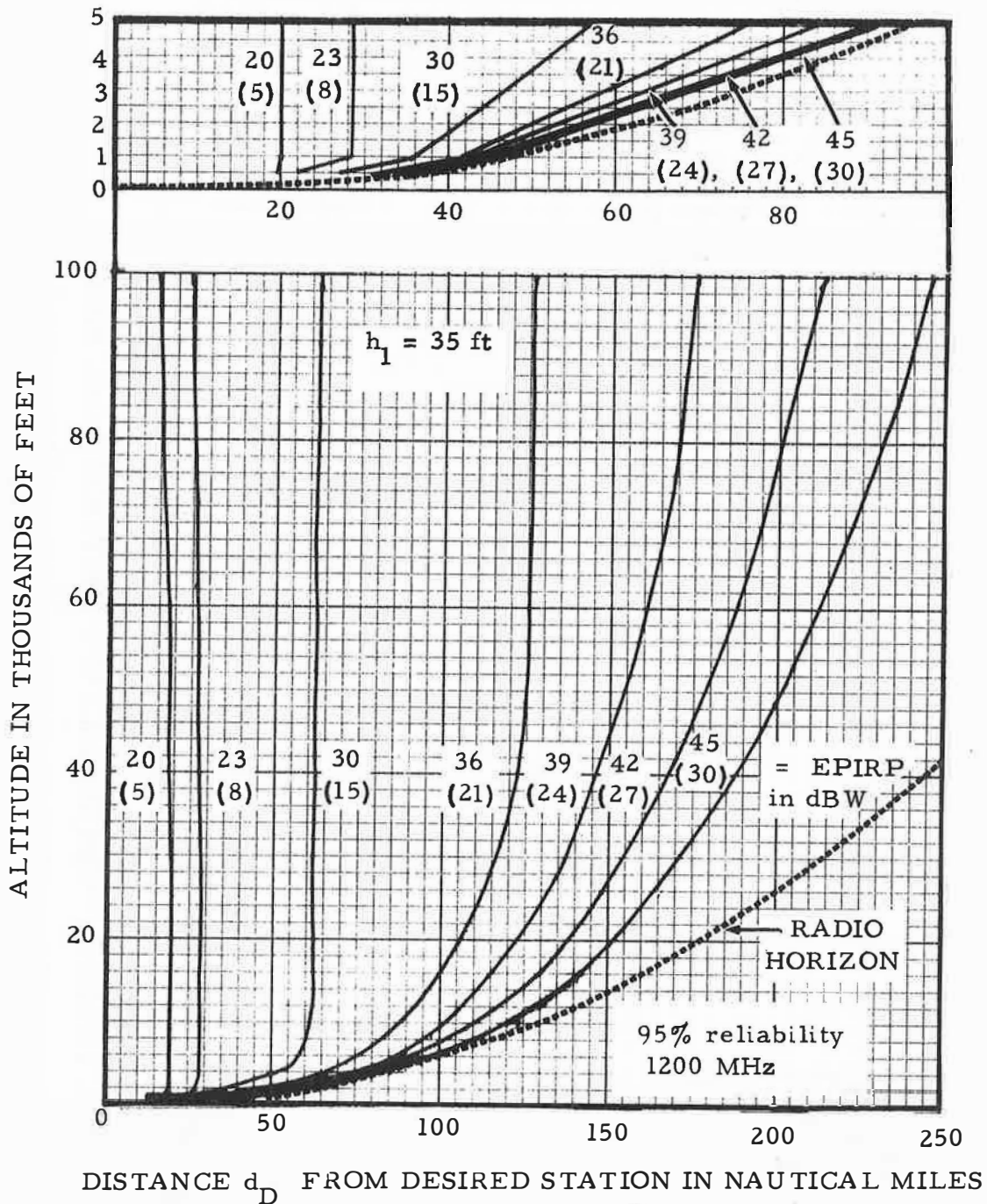


Figure 22. Service volumes without interference; 1200 MHz, isotropic antenna, 69/70/70. EIRP's required for -109 dBW (equivalent to -86 dBW/m^2) at an isotropic airborne receiving antenna (ground-to-air) are given along with those, in parentheses, required for -124 dBW (equivalent to -101 dBW/m^2) at an isotropic ground facility receiving antenna (air-to-ground).

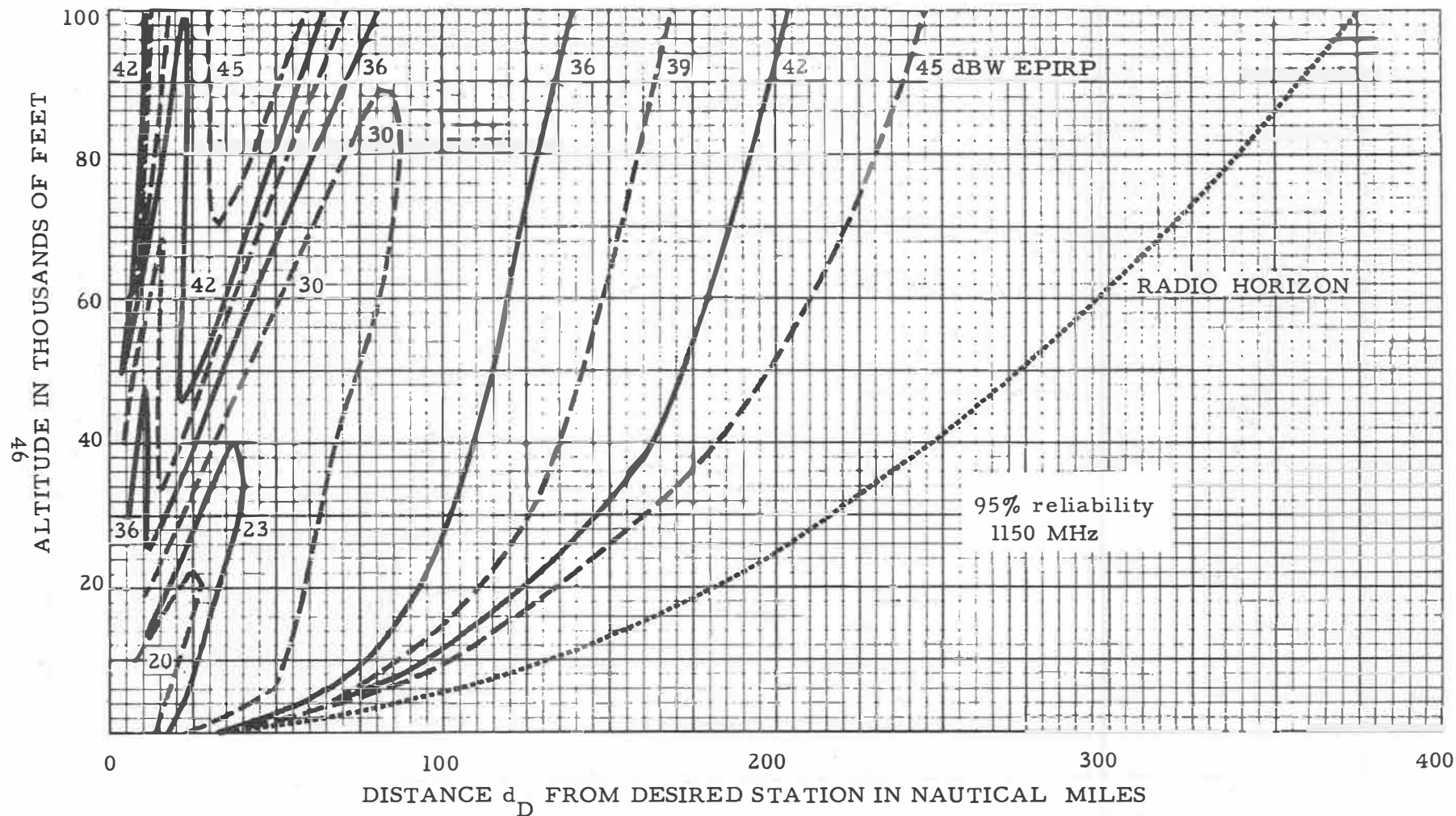


Figure 23. Service volumes without interference; TACAN, RTA-2, $62\Delta G/70/67$. The reference power of -106 dBW is equivalent to a power density of -86 dBW/m². The effective peak isotropic radiated power (EPIRP) required to produce -106 dBW of available power from a reference half-wave dipole located on the service volume boundary is given for each curve.

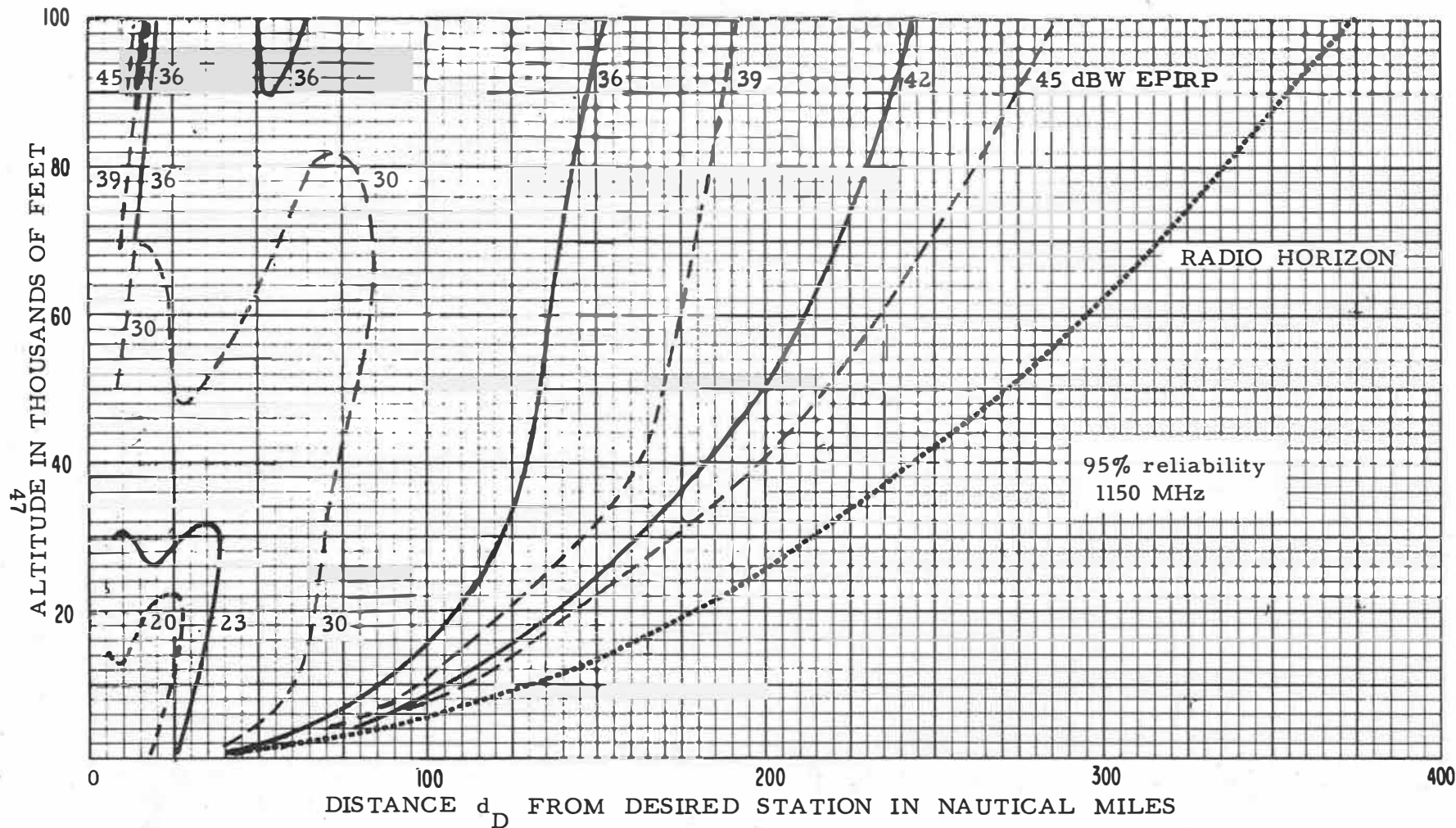


Figure 24. Service volumes without interference; TACAN, URN-3, 62/62/67. The reference power of -106 dBW is equivalent to a power density of -86 dBW/m². The effective peak isotropic radiated power (EPIRP) required to produce -106 dBW of available power from a reference half-wave dipole located on the service volume boundary is given for each curve.

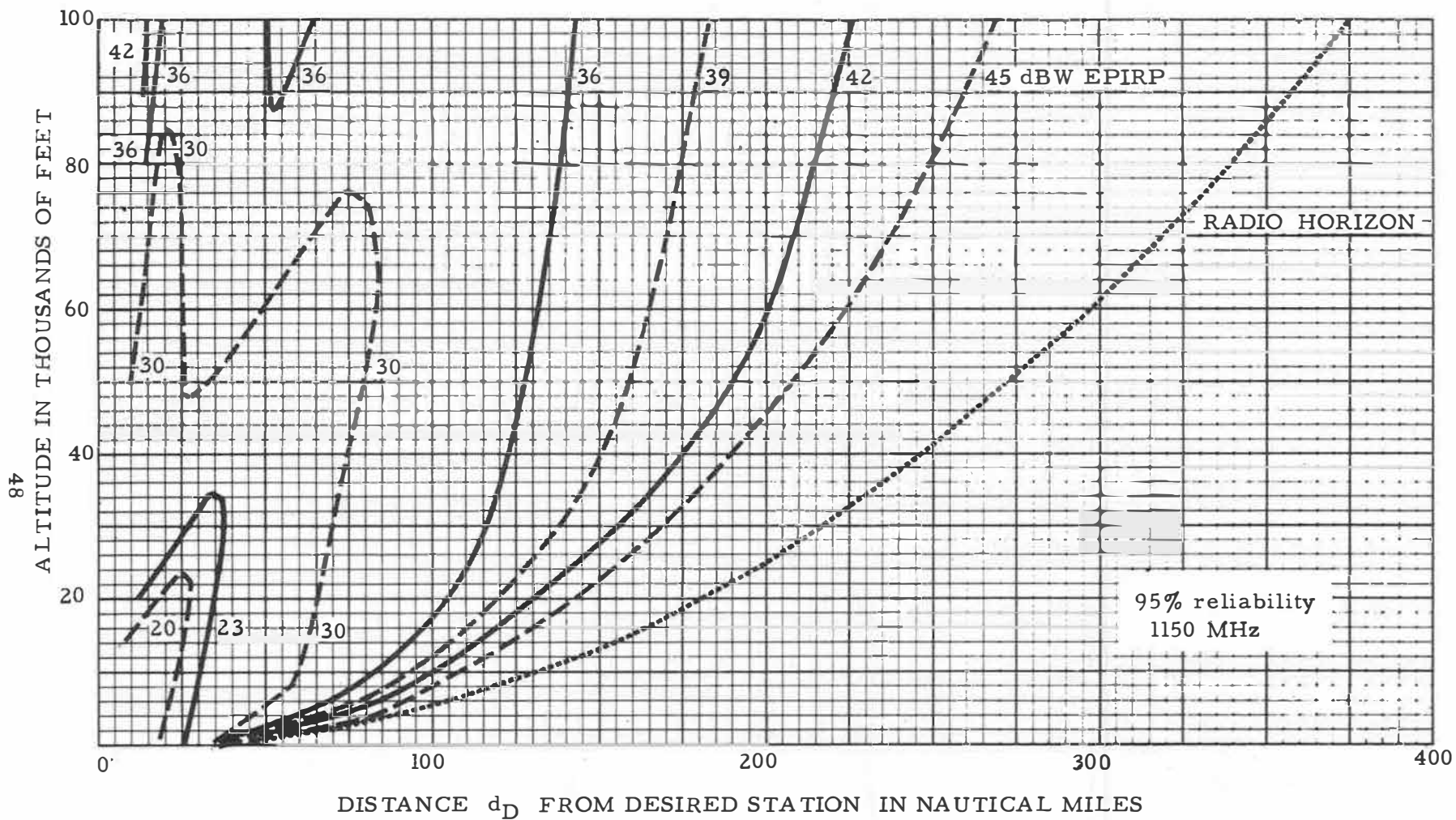


Figure 25. Service volumes without interference; TACAN, URN-3, 62/70/67. The reference power of -106 dBW is equivalent to a power density of -86 dBW/m². The effective peak isotropic radiated power (EPIRP) required to produce -106 dBW of available power from a reference half-wave dipole located on the service volume boundary is given for each curve.

$h_1 = 16$ ft above ground, 4 ft above the counterpoise.

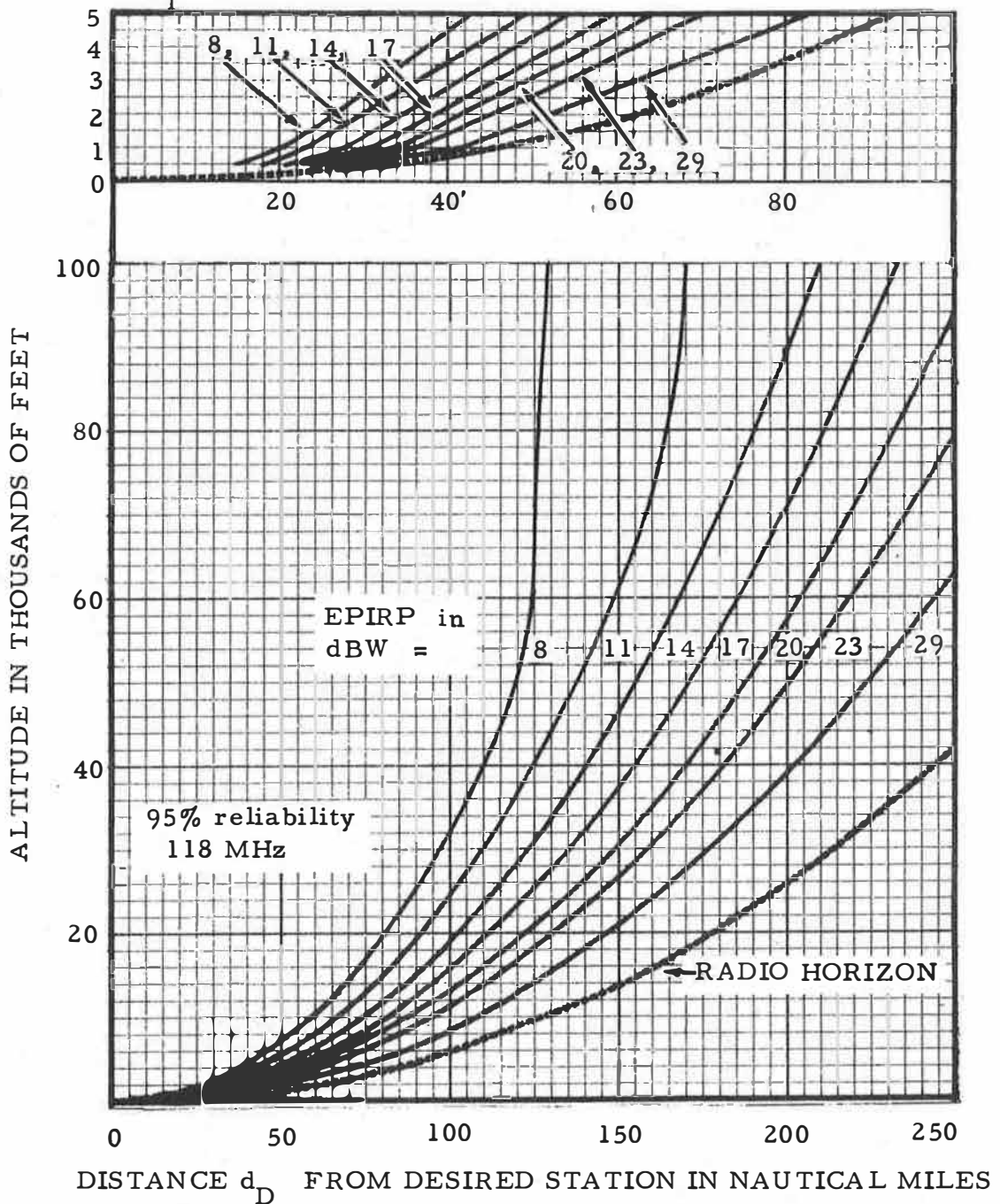


Figure 26. Service volumes without interference; 118 MHz, isotropic antenna, 69/70/67. EPIRP's required for -114 dBW (equivalent to -111 dBW/m²) at an isotropic airborne receiving antenna are given.

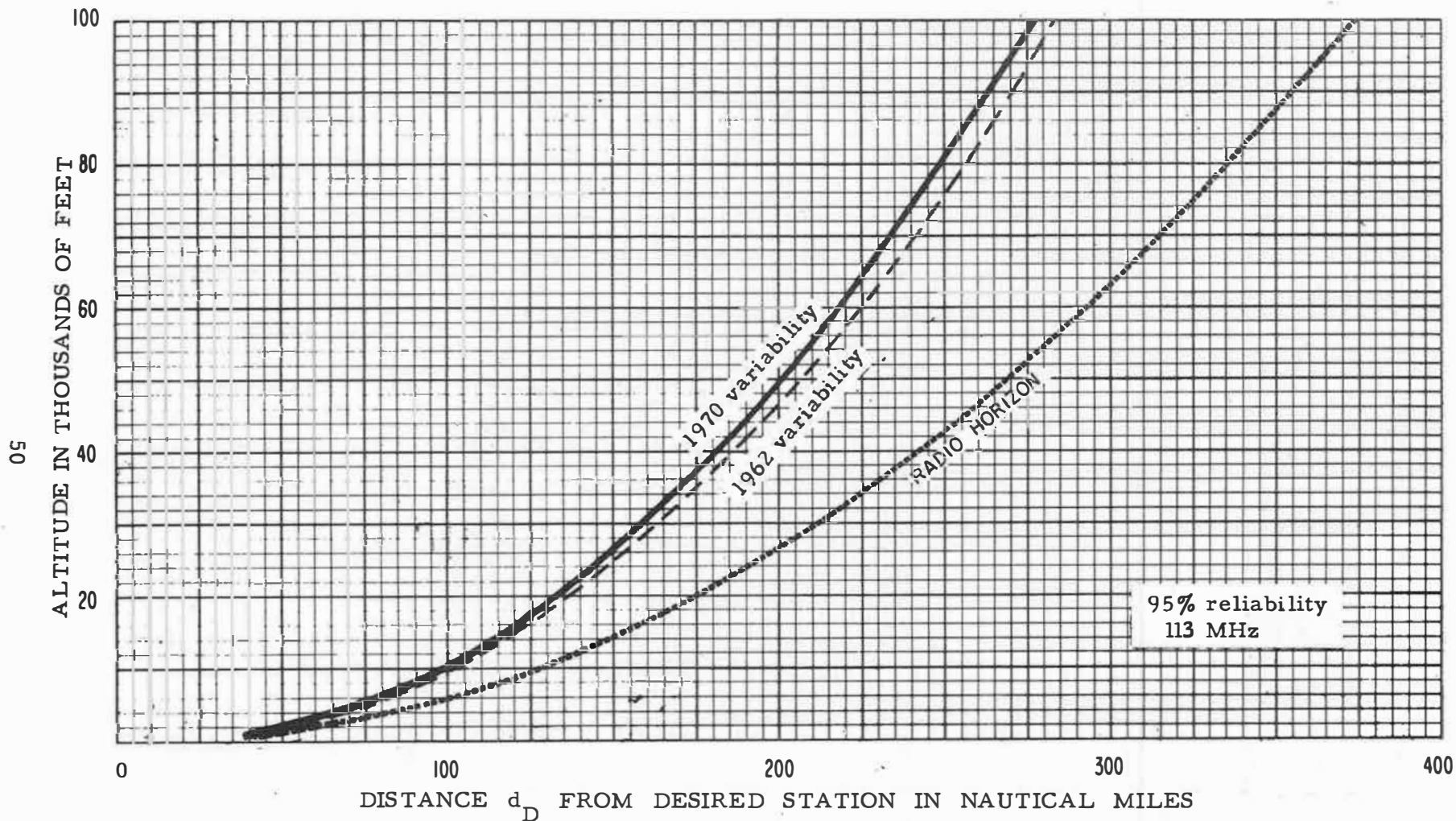


Figure 27. Service volumes without interference; VOR, 4-loop, 62/62-70/67. The -112 dBW reference power is equivalent to a power density of -112 dBW/m^2 . 20 dBW of radiated power (22.15 dB EIRP) is required to provide -112 dBW of available power from a reference half-wave dipole located on the service volume boundary.

7. REFERENCES

- Airborne Instrument Laboratory, AIL solid-state ILS, types 55-E and 55-F (proposal).
- Barghausen, A.F., A.P. Barsis, B.R. Bean, H.F. Dougherty, E.J. Dutton, E.F. Florman, F.O. Guiraud, J.D. Horn, R.S. Kirby, A.G. Longley, L.J. Maloney, R.E. McGavin, S. Murahata, P.L. Rice, L.P. Riggs, J.J. Tary, and R.W. Wilber (1961), Ground telecommunication performance standards, Part 5, Tropospheric systems, unpublished¹ NBS Rept. (Later published as U.S. Air Force Technical Order 31Z-10-1).
- Barsis, A.P., G.D. Gierhart, F.M. Capps, and E.M. Gray (1970), Air-ground radio wave propagation measurements in the 820-to 850-MHz frequency range (to be published).
- CCIR (1962), Tropospheric wave transmission loss prediction, study document V/23-E for question 185(V) of study program 138(V).
- FAA (1963), TACAN ground station equipment, FAA specification FAA-E-2006.
- FAA (1967), DME ground station equipment, FAA specification FAA-E-2266.
- Gierhart, G.D. (1963), Service volume predictions for air navigation facilities, unpublished¹ NBS Rept.
- Gierhart, G.D. (1964), Service volume predictions for air navigation facilities, unpublished¹ NBS Rept.

¹

These documents are in the public domain since they were issued as official Government writing. However, they are considered unpublished since they were not printed for wide public distribution.

- Gierhart, G.D., and M.E. Johnson (1965), Interference predictions for the instrument landing system, NBS Tech. Note 324 (\$0.30²).
- Gierhart, G.D., and M.E. Johnson (1967), Interference predictions for VHF/UHF air navigation aids, ESSA Tech. Rept. IER 26-ITSA 26 (AD 654 924³).
- Gierhart, G.D., and M.E. Johnson (1969a), Interference predictions for VHF/UHF air navigation aids (companion report to IER 26-ITSA 26), ESSA Tech. Rept. ERL 138-ITS 95 (\$0.60²).
- Gierhart, G.D., and M.E. Johnson (1969b), Transmission loss atlas for select aeronautical service bands from 0.125 to 15.5 GHz, ESSA Tech. Rept. ERL 111-ITS 79 (\$1.25²).
- Gierhart, G.D., J.S. Miller, M.E. Johnson, and A.P. Barsis (1962), The prediction of service volumes for air navigation facilities, unpublished¹ NBS Rept.
- Gierhart, G.D., R.W. Hubbard, and D.V. Glen (1970), Electro-space planning and engineering for the air traffic environment, DoT Tech. Rept. FAA-RD-70-71 (\$2.25²).
- Hollm, E.R. (April 2, 1968), letter to Mr. R. Johnson of FAA.
- Johnson, M.E. (1967), Computer programs for tropospheric transmission loss calculations, ESSA Tech. Rept. IER 45-ITSA 45 (\$1.00²).

² Copies of these reports are sold for the indicated price by the Superintendent of Documents, U.S. Government Printing Office, Washington, D.C. 20402.

³ Copies of these reports are sold for \$3.00 each (\$0.95 microfiche) by the National Technical Information Service, Operations Division, Springfield, Va. 22151. Order by using the indicated accession number.

Longley, A.G., and P.L. Rice (1968), Prediction of tropospheric radio transmission loss over irregular terrain, a computer method -- 1968, ESSA Tech. Rept. ERL 79-ITS 67 (\$0.70², AD 676 874³).

Longley, A.G., and R.K. Reasoner (1970), Comparison of propagation measurements with predicted values in the 20 to 10,000 MHz range, ESSA Tech. Rept. ERL 148-ITS 97 (\$1.00).

Rice, P.L., A.G. Longley, K.A. Norton, and A.P. Barsis (1967), Transmission loss predictions for tropospheric communication circuits, NBS Tech. Note 101, Vols. I and II, revised (AD 687 820 and AD 687 821³).

Wilcox, Abstract of technical data, Wilcox model 412 solid state ILS.

APPENDIX A. ERRATA FOR PREVIOUS REPORTS
A.1 ESSA Technical Report IER 26-ITSA 26.
(Gierhart and Johnson, 1967)

Page 29 Replace the label "EPRP = 30 dBW" with the label "EPRP = 39 dBW."

Pages 35-37 Replace figures 11 through 13 with figures A.1 through A.3 given here. One of the programs used to calculate the previous curves was run with a missing or misplaced card. An indication of a possible problem occurred while developing curves for Gierhart and Johnson (1969a, fig. 15) and, in fact, figure A.3 was made up from the 1969 calculations. The new curves are usually within 2 dB of the previous curves, but the difference can be as high as 3.5 dB.

Page 53 Replace figure 27 with figure A.4 given here. The placement of station separation labels for values less than 60 nm has been altered in order to make the correspondence between curves and labels more definitive.

A.2 ESSA Technical Report ERL 111-ITS 79.
(Gierhart and Johnson, 1969b)

The "F" used in many figure captions to indicate frequency is not defined in the list of symbols.

Page 88 The "HGz" in the caption of figure 88 should be changed to "GHz".

Page 123 The "130" in (B-6) should be changed to "130 d".

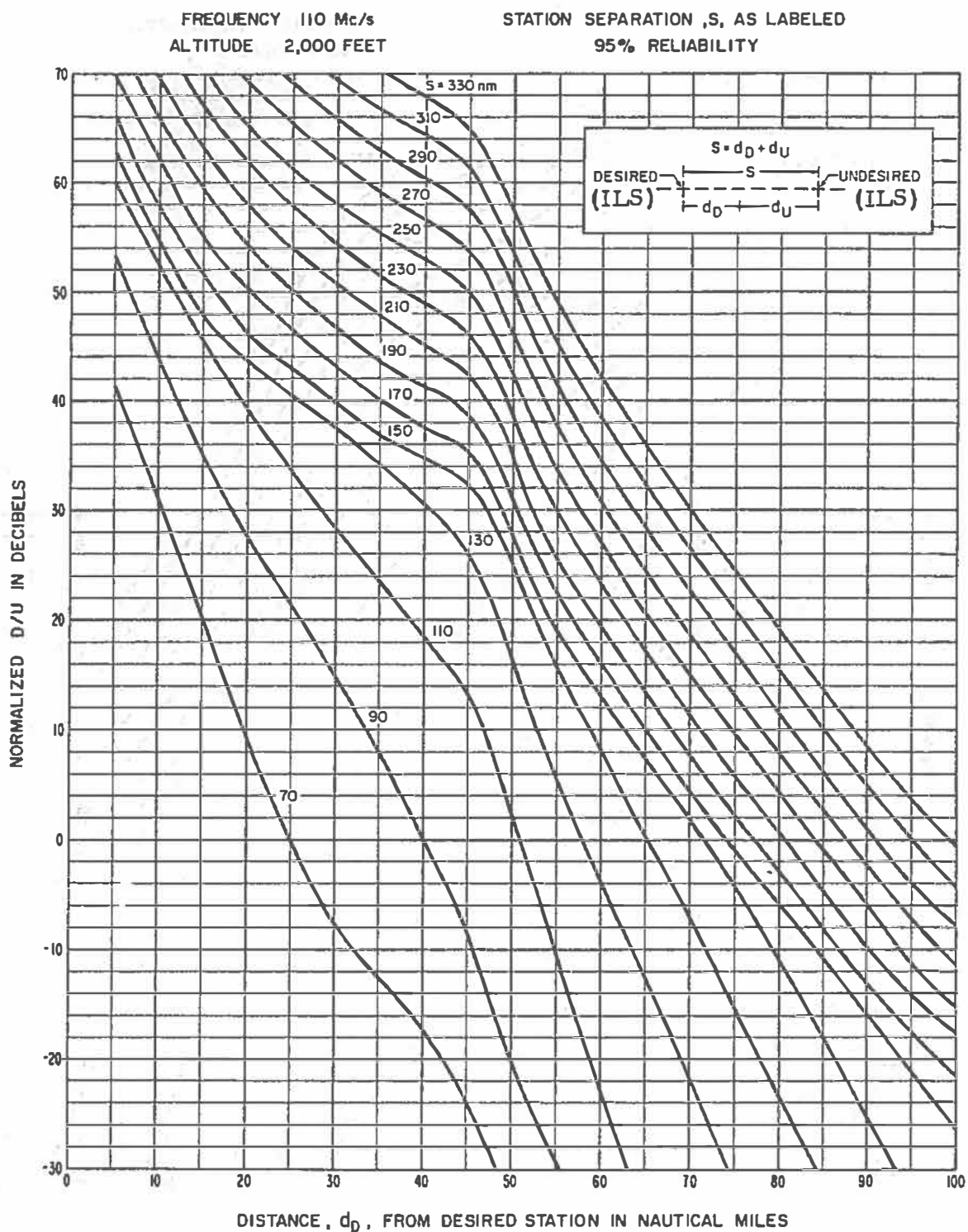


Figure A.1. Normalized D/ U for co-channel ILS localizers; altitude = 2,000 ft. . A replacement for Gierhart and Johnson (1967, fig. 11).

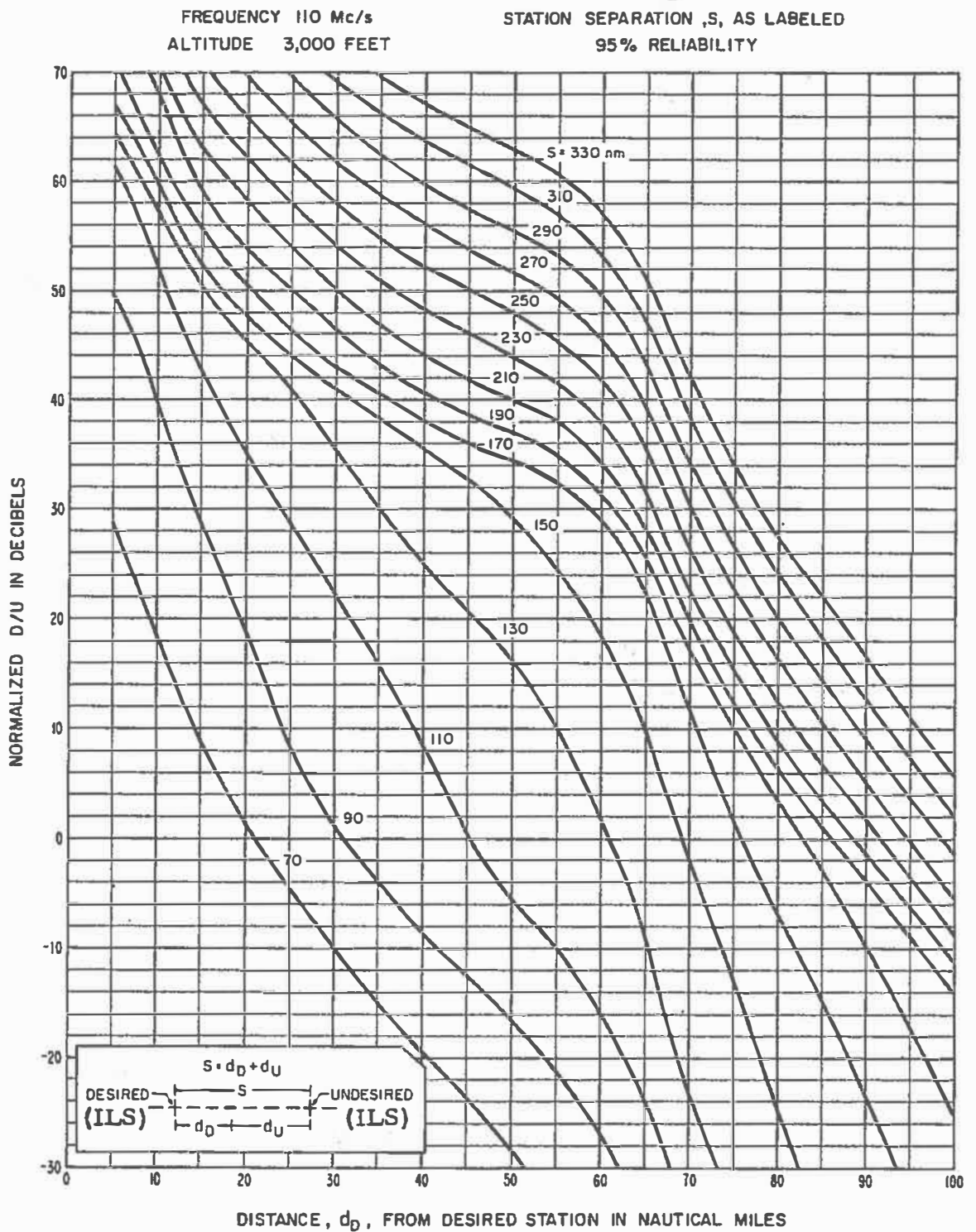


Figure A. 2. Normalized D/ U for co-channel ILS localizers; altitude = 3,000 ft. . A replacement for Gierhart and Johnson (1967, fig. 12).

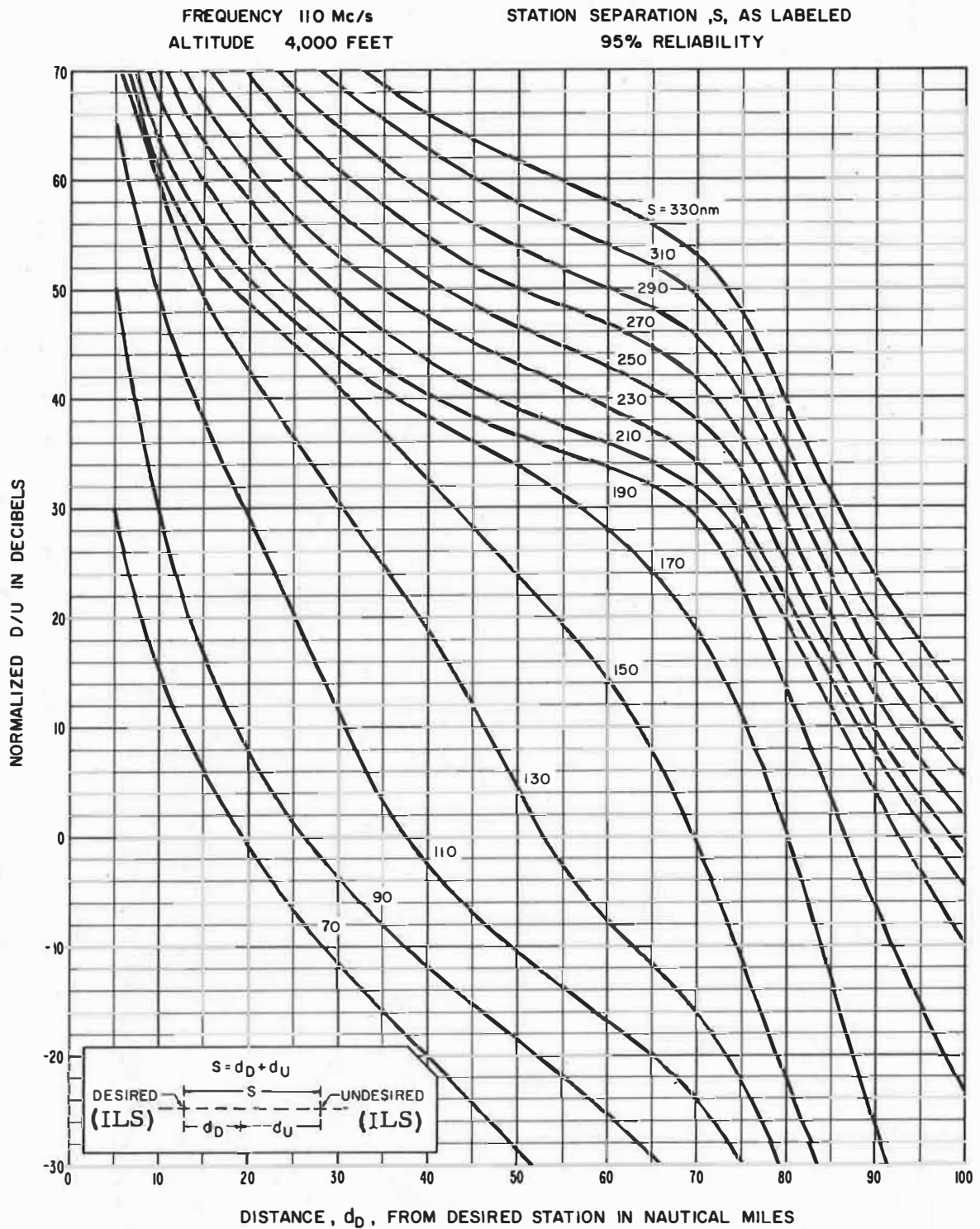


Figure A. 3. Normalized D/U for co-channel ILS localizers; altitude = 4,000 ft.,. A replacement for Gierhart and Johnson (1967, fig. 13).

FREQUENCY 113 Mc/s
 D/U (95) = 32 dB

STATION SEPARATION, S, AS LABELED
 95 % RELIABILITY

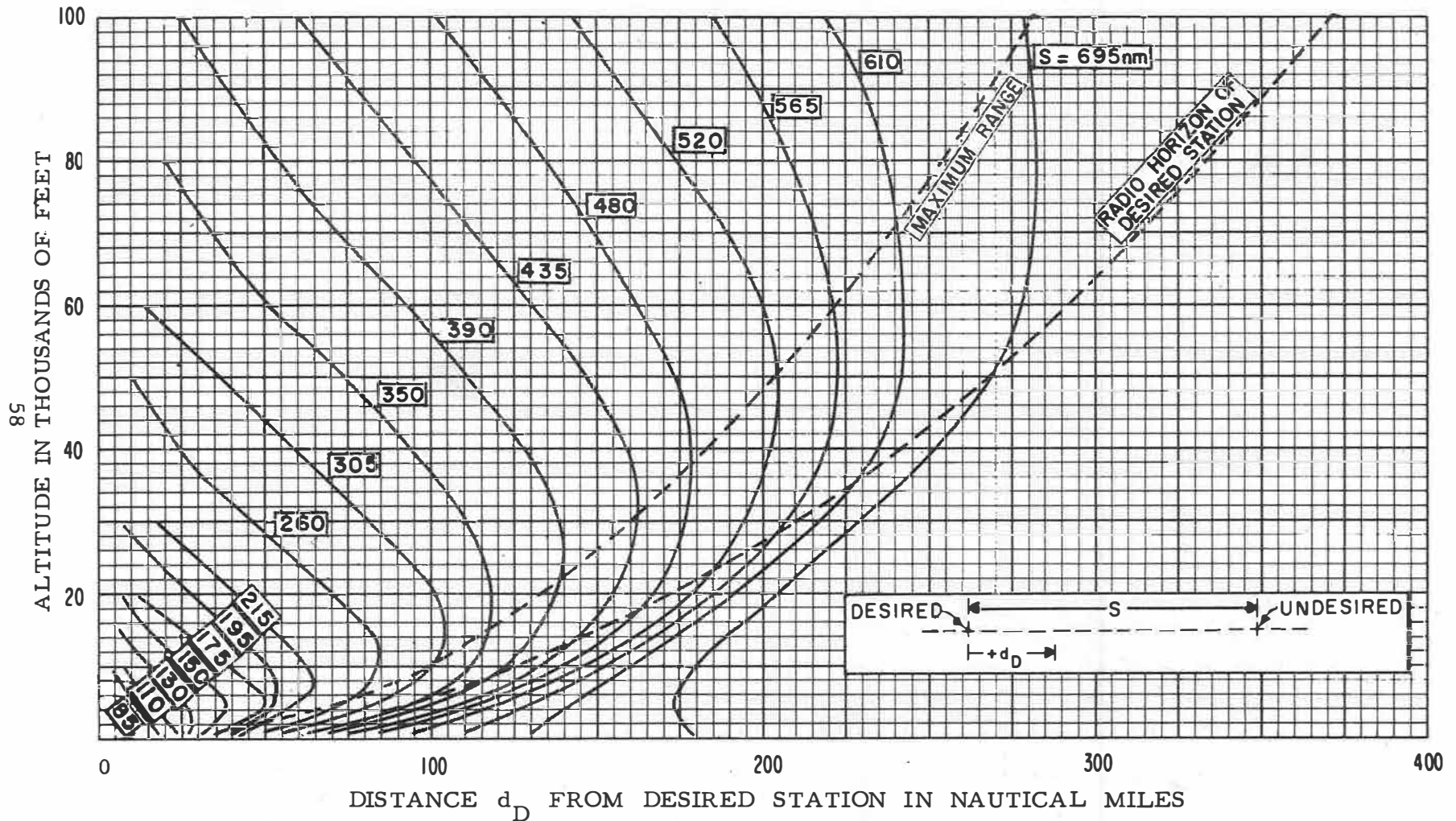


Figure A. 4. Service volumes for VOR; D/U(95) = 32 dB. A replacement for Gierhart and Johnson (1967, fig. 27).